

# Topological Charged Black Holes in High Dimensional Spacetimes and Their Formation from Gravitational Collapse of a Type II Fluid

Yumei Wu<sup>\* 1</sup>, M. F. A. da Silva<sup>† 2</sup>, N. O. Santos<sup>‡ 3,4</sup>, and Anzhong Wang<sup>§ 2,5,6</sup>

<sup>1</sup> *Instituto de Matemática, Universidade Federal do Rio de Janeiro, Caixa Postal 68530, CEP. 21945 – 970, Rio de Janeiro – RJ, Brazil*

<sup>2</sup> *Departamento de Física Teórica, Universidade do Estado do Rio de Janeiro, Rua São Francisco Xavier 524, Maracanã, CEP. 20550 – 013, Rio de Janeiro – RJ, Brazil*

<sup>3</sup> *Laboratório Nacional de Computação Científica, CEP. 25651 – 070, Petrópolis-RJ, Brazil*

<sup>4</sup> *Centro Brasileiro de Pesquisas Físicas, CEP. 22290 – 180, Rio de Janeiro-RJ, Brazil*

<sup>5</sup> *CASPER, Physics Department, P.O. Box 97316, Baylor University, Waco, TX76798-7316*

<sup>6</sup> *Department of Physics, University of Illinois at Urbana-Champaign, 1110 West Green Street, Urbana, IL 61801-3080*  
(November 2, 2021)

Topological charged black holes coupled with a cosmological constant in  $R^2 \times X^{D-2}$  spacetimes are studied, where  $X^{D-2}$  is an Einstein space of the form  ${}^{(D-2)}R_{AB} = k(D-3)h_{AB}$ . The global structure for the four-dimensional spacetimes with  $k = 0$  is investigated systematically. The most general solutions that represent a Type II fluid in such a high dimensional spacetime are found, and showed that topological charged black holes can be formed from the gravitational collapse of such a fluid. When the spacetime is (asymptotically) self-similar, the collapse always forms black holes for  $k = 0, -1$ , in contrast to the case  $k = 1$ , where it can form either black holes or naked singularities.

## I. INTRODUCTION

Lately black holes in high dimensions have attracted a great deal of attention in the gravity-gauge theory correspondence [1], and been further promoted by theories of TeV gravity, in which high dimensional black holes are predicted to be produced in the next generation of colliders [2].

In black hole physics, one of the fundamental features is the topology of a black hole. In four-dimensional asymptotically flat stationary spacetimes, Hawking first showed that a black hole has necessarily a  $S^2$  topology, provided that the dominant energy condition holds [3]. Later, it was realized that Hawking's theorem can be improved in various aspects, see [4] and references therein. However, once the energy condition is relaxed, a black hole can have quite different topologies. Such examples can occur even in  $3 + 1$  dimensional spacetimes where the cosmological constant is negative [5]. In high dimensional spacetimes, it was found that even if the energy conditions hold, the topology is still not unique. In particular, a five-dimensional rotating vacuum black hole can have either a  $S^3$  topology [6], or a  $S^2 \times S^1$  topology [7], although a static charged dilaton black hole in high dimensional asymptotically flat spacetimes indeed has a unique topology, which is a  $(D - 2)$ -sphere [8]. When the cosmological constant is different from zero, similar to the four-dimensional case, static black holes can have different topologies [9].

In this paper we shall study the formation of topological black holes from gravitational collapse of a type II fluid in high dimensional spacetimes. Specifically, the paper is organized as follows: In Sec. II we present a general  $R^2 \times X^{D-2}$  decomposition. In Sec. III, assuming that  $X^{D-2}$  is an Einstein space with a constant curvature,  ${}^{(D-2)}R_{AB} = k_D h_{AB}$ , we re-derive the charged solutions coupled with a cosmological constant in any dimensional spacetimes, without assuming that the spacetime is static. In Sec. IV we systematically study the global structure for the case  $D = 4$  and  $k_D = 0$ , while in Sec. V, all the type II fluid solutions in D-dimensional spacetimes are given. In Sec. VI we study the formation of topological charged and uncharged black holes from the gravitational collapse of such a fluid, while in Sec. VII our main conclusions are summarized. There is also an appendix, in which trapped surfaces and apparent horizons are defined.

Before proceeding further, we would like to note that the formation of topological black holes from gravitational collapse in four-dimensional spacetimes was studied in [10], while gravitational collapse in high dimensional spherically symmetric spacetimes was investigated in [11].

---

\*E-mail: yumei@dmm.im.ufrj.br

†E-mail: mfas@dtf.if.uerj.br

‡E-mail: nos@cbpf.br

§E-mail: Anzhong\_Wang@baylor.edu

## II. $R^2 \times X^{D-2}$ DECOMPOSITION

In this paper let us consider a D-dimensional spacetime described by the metric

$$ds^2 = g_{\mu\nu} dx^\mu dx^\nu = \gamma_{ab}(x^c) dx^a dx^b + s^2(x^c) h_{AB}(x^C) dx^A dx^B, \quad (2.1)$$

where we use Greek indices, such as,  $\mu, \nu, \lambda$ , to run from 0 to  $D-1$ , lowercase Latin indices, such as,  $a, b, c, \dots$ , to run from 0 to 1, and uppercase Latin indices, such as,  $A, B, C, \dots$ , to run from 2 to  $D-1$ . Clearly, the above metric is invariant under the coordinate transformations,

$$x^a = x^a(x'^b), \quad x^A = x^A(x'^B). \quad (2.2)$$

Introducing the quantities  $\gamma^{ab}(x^c)$  and  $h^{AB}(x^C)$  via the relations,

$$\gamma^{ac}\gamma_{cb} = \delta_b^a, \quad h^{AC}h_{CB} = \delta_B^A, \quad (2.3)$$

we find that

$$g_{\mu\nu} = \begin{pmatrix} \gamma_{ab} & 0 \\ 0 & s^2 h_{AB} \end{pmatrix}, \quad g^{\mu\nu} = \begin{pmatrix} \gamma^{ab} & 0 \\ 0 & s^{-2} h^{AB} \end{pmatrix}. \quad (2.4)$$

Then, the non-vanishing Christoffel symbols are given by

$$\begin{aligned} {}^{(D)}\Gamma_{bc}^a &= {}^{(2)}\Gamma_{bc}^a, & {}^{(D)}\Gamma_{AB}^a &= -h_{AB} s s^{,a}, \\ {}^{(D)}\Gamma_{aB}^A &= s^{-1} s_{,a} \delta_B^A, & {}^{(D)}\Gamma_{BC}^A &= {}^{(n)}\Gamma_{BC}^A, \end{aligned} \quad (2.5)$$

where  $s_{,a} \equiv \partial s / \partial x^a$ ,  $s^{,a} \equiv \gamma^{ab} s_{,b}$ ,  ${}^{(2)}\Gamma_{bc}^a$  and  ${}^{(n)}\Gamma_{BC}^A$  are the Christoffel symbols calculated, respectively, from  $\gamma_{ab}(x^c)$  and  $h^{AB}(x^C)$ , and  $n \equiv D-2$ . From Eq.(2.5) we find that the Ricci tensor, defined by,

$${}^{(D)}R_{\mu\nu} = {}^{(D)}\Gamma_{\mu\nu,\lambda}^\lambda - {}^{(D)}\Gamma_{\lambda\mu,\nu}^\lambda + {}^{(D)}\Gamma_{\lambda\sigma}^\lambda {}^{(D)}\Gamma_{\mu\nu}^\sigma - {}^{(D)}\Gamma_{\sigma\nu}^\lambda {}^{(D)}\Gamma_{\lambda\mu}^\sigma, \quad (2.6)$$

has the following non-vanishing components,

$$\begin{aligned} {}^{(D)}R_{ab} &= {}^{(2)}R_{ab} - \frac{D-2}{s} \nabla_a \nabla_b s, \\ {}^{(D)}R_{AB} &= {}^{(n)}R_{AB} - [s \square s + (D-3) (\nabla_c s) (\nabla^c s)] h_{AB}, \end{aligned} \quad (2.7)$$

where  $\square \equiv \gamma^{ab} \nabla_a \nabla_b$ , and  $\nabla_a$  denotes the covariant derivative with respect to  $\gamma_{ab}$ .

To calculate  ${}^{(2)}R_{ab}$ , we first note that the Riemann tensor  ${}^{(2)}R_{abcd}$  has only one independent component, say,  ${}^{(2)}R_{0101}$ . Then, in terms of  ${}^{(2)}R_{0101}$  we have

$$\begin{aligned} {}^{(2)}R_{abcd} &= {}^{(2)}R_{0101} (\delta_a^0 \delta_b^1 \delta_c^0 \delta_d^1 - \delta_a^0 \delta_b^1 \delta_c^1 \delta_d^0 - \delta_a^1 \delta_b^0 \delta_c^0 \delta_d^1 + \delta_a^1 \delta_b^0 \delta_c^1 \delta_d^0), \\ {}^{(2)}R_{ab} &\equiv {}^{(2)}R^c{}_{acb} = {}^{(2)}R_{0101} (\gamma^{11} \delta_a^0 \delta_b^0 - \gamma^{01} (\delta_a^0 \delta_b^1 + \delta_a^1 \delta_b^0) + \gamma^{00} \delta_a^1 \delta_b^1). \end{aligned} \quad (2.8)$$

On the other hand, for the second block of the metric, we shall consider only the case where  $h_{AB}$  represents a  $n$ -dimensional surface with constant curvature,

$${}^{(n)}R_{AB} = k_D h_{AB}(x^C), \quad (2.9)$$

where, without loss of generality, one can always set  $k_D = (D-3)k$  with  $k = -1, 0, 1$ . Then the surfaces of constant  $x^a$  will be referred, respectively, to as *hyperbolic*, *flat* and *elliptic*.

## III. TOPOLOGICAL CHARGED BLACK HOLES COUPLED WITH THE COSMOLOGICAL CONSTANT

Using the gauge freedom of Eq.(2.2), in this section we shall choose the coordinates such that

$$\gamma_{tr}(x^c) = 0, \quad s(x^c) = r, \quad (3.1)$$

where  $x^c = \{t, r\}$ . This will be referred to as *the Schwarzschild gauge*. Then, we find that

$$ds^2 = -e^{2\Phi(t,r)} dt^2 + e^{2\Psi(t,r)} dr^2 + r^2 h_{AB}(x^C) dx^A dx^B. \quad (3.2)$$

For such a form, there still remains the gauge freedom

$$t = t(\bar{t}). \quad (3.3)$$

Later, we shall use it to fix some integration functions. For the metric (3.2) we find

$$\begin{aligned} {}^{(2)}R_{ab} &= -\frac{1}{2} {}^{(2)}R (e^{2\Phi} \delta_a^0 \delta_b^0 - e^{2\Psi} \delta_a^1 \delta_b^1), \\ {}^{(2)}R &= 2 \{ e^{-2\Phi} [\Psi_{,tt} + \Psi_{,t}(\Psi_{,t} - \Phi_{,t})] - e^{-2\Psi} [\Phi_{,rr} + \Phi_{,r}(\Phi_{,r} - \Psi_{,r})] \}. \end{aligned} \quad (3.4)$$

It can be also shown that

$$\begin{aligned} \nabla_a \nabla_b r &= -e^{2(\Phi-\Psi)} \Phi_{,r} \delta_a^0 \delta_b^0 - \Psi_{,t} (\delta_a^0 \delta_b^1 + \delta_a^1 \delta_b^0) - \Psi_{,r} \delta_a^1 \delta_b^1, \\ \square r &= e^{-2\psi} (\Phi_{,r} - \Psi_{,r}). \end{aligned} \quad (3.5)$$

Substituting Eqs.(2.9), (3.4) and (3.5) into Eq.(2.7) we obtain

$$\begin{aligned} {}^{(D)}R_{00} &= -[\Psi_{,tt} + \Psi_{,t}(\Psi_{,t} - \Phi_{,t})] \\ &\quad + e^{2(\Phi-\Psi)} \left[ \Phi_{,rr} + \Phi_{,r} \left( \Phi_{,r} - \Psi_{,r} + \frac{D-2}{r} \right) \right], \end{aligned} \quad (3.6)$$

$${}^{(D)}R_{01} = \frac{D-2}{r} \Psi_{,t}, \quad (3.7)$$

$$\begin{aligned} {}^{(D)}R_{11} &= e^{2(\Psi-\Phi)} [\Psi_{,tt} + \Psi_{,t}(\Psi_{,t} - \Phi_{,t})] \\ &\quad - \left( \Phi_{,rr} + \Phi_{,r}(\Phi_{,r} - \Psi_{,r}) - \frac{D-2}{r} \Psi_{,r} \right), \end{aligned} \quad (3.8)$$

$${}^{(D)}R_{AB} = \{ k_D - [r(\Phi_{,r} - \Psi_{,r}) + (D-3)] e^{-2\Psi} \} h_{AB}. \quad (3.9)$$

On the other hand, the D-dimensional Einstein-Maxwell equations with the cosmological constant,  $\Lambda_D$ , read

$${}^{(D)}R_{\mu\nu} - \frac{1}{2} g_{\mu\nu} {}^{(D)}R = 8\pi G_D {}^{(D)}E_{\mu\nu} - \Lambda_D g_{\mu\nu}, \quad (3.10)$$

where the energy-momentum tensor  ${}^{(D)}E_{\mu\nu}$  is given by

$${}^{(D)}E_{\mu\nu} = \frac{1}{4\pi G_D} \left( {}^{(D)}F_{\mu\alpha} {}^{(D)}F_{\nu}{}^{\alpha} - \frac{1}{4} g_{\mu\nu} {}^{(D)}F_{\alpha\beta} {}^{(D)}F^{\alpha\beta} \right), \quad (3.11)$$

with the electromagnetic field  ${}^{(D)}F_{\mu\nu}$  satisfying the Maxwell equations,

$$D^\nu {}^{(D)}F_{\mu\nu} = 0, \quad (3.12)$$

where  $D_\nu$  denotes the covariant derivative with respect to the D-dimensional metric  $g_{\mu\nu}$ . From the symmetry of the spacetime, without loss of generality, we can always assume that  ${}^{(D)}F_{\mu\nu}$  is function of  $t$  and  $r$  only, and takes the form,

$${}^{(D)}F_{\mu\nu} = F(t, r) (\delta_\mu^0 \delta_\nu^1 - \delta_\mu^1 \delta_\nu^0). \quad (3.13)$$

Substituting Eqs.(3.11) and (3.12) into Eq.(3.10) we find that

$$\begin{aligned} {}^{(D)}R_{\mu\nu} &= F^2 \left( 2 (e^{-2\Psi} \delta_\mu^0 \delta_\nu^0 - e^{-2\Phi} \delta_\mu^1 \delta_\nu^1) + \frac{2}{D-2} e^{-2(\Phi+\Psi)} g_{\mu\nu} \right) \\ &\quad + \frac{2\Lambda_D}{D-2} g_{\mu\nu}. \end{aligned} \quad (3.14)$$

Combining Eq.(3.7) with the above equation, we obtain

$$\Psi(t, r) = \Psi(r). \quad (3.15)$$

On the other hand, from the Maxwell field equation (3.12) we have

$$F(t, r) = \frac{C_0}{r^{D-2}} e^{\Phi+\Psi}, \quad (3.16)$$

where  $C_0$  is an integration constant. Inserting Eqs.(3.15) and (3.16) into Eqs.(3.6)-(3.9), we find the following independent equations,

$$\Phi_{,rr} + \Phi_{,r} \left( \Phi_{,r} - \Psi_{,r} + \frac{D-2}{r} \right) = e^{2\Psi} \left( \frac{C_1}{r^{2(D-2)}} - \frac{2\Lambda_D}{D-2} \right), \quad (3.17)$$

$$\Phi_{,rr} + \Phi_{,r} (\Phi_{,r} - \Psi_{,r}) - \frac{D-2}{r} \Psi_{,r} = e^{2\Psi} \left( \frac{C_1}{r^{2(D-2)}} - \frac{2\Lambda_D}{D-2} \right), \quad (3.18)$$

$$k_D e^{2\Psi} - r (\Phi_{,r} - \Psi_{,r}) - (D-3) = e^{2\Psi} \left( \frac{C_1}{(D-3)r^{2(D-3)}} + \frac{2\Lambda_D}{D-2} r^2 \right), \quad (3.19)$$

where  $C_1 \equiv 2(D-3)C_0^2/(D-2)$ . From Eqs.(3.17) and (3.18) we obtain

$$\Phi(t, r) = -\Psi(r) + \Phi_0(t), \quad (3.20)$$

where  $\Phi_0(t)$  is an arbitrary function. However, using the coordinate transformation (3.3), we can always set  $\Phi_0(t) = 0$ , a condition that will be assumed below. Then, substituting the above expression into Eq.(3.19) and integrating it, we obtain

$$\Phi = -\Psi = \frac{1}{2} \ln \left( k - \frac{2M}{r^{D-3}} + \frac{Q^2}{r^{2(D-3)}} - \Lambda r^2 \right), \quad (3.21)$$

where

$$\Lambda \equiv \frac{2\Lambda_D}{(D-1)(D-2)}, \quad (3.22)$$

and  $M$  and  $Q$  are two arbitrary constants, related to the total mass  $M_D$  and charge  $Q_D$  of the spacetime via the relations [12],

$$M = \frac{8\pi G_D M_D}{(D-2)A_\Sigma}, \quad Q = \frac{4\pi G_D Q_D}{A_\Sigma}, \quad (3.23)$$

where  $A_\Sigma$  denotes the total area of the  $(D-2)$ -dimensional surface spanned by  $h_{AB}$ ,

$$A_\Sigma = \int \sqrt{h} d^{D-2}x. \quad (3.24)$$

It can be shown that the solution (3.21) also satisfies Eqs.(3.17) and (3.18), with the electromagnetic field given by

$${}^{(D)}F_{\mu\nu} = \left( \frac{(D-2)(D-3)}{2} \right)^{1/2} \frac{Q}{r^{D-2}} (\delta_\mu^0 \delta_\nu^1 - \delta_\mu^1 \delta_\nu^0). \quad (3.25)$$

When the surfaces of constant  $t$  and  $r$  are not compact, clearly  $A_\Sigma$  becomes infinity, so do  $M_D$  and  $Q_D$ . However, one can still keep the quantities  $m$  and  $q$  finite, where

$$m \equiv \frac{M_D}{A_\Sigma}, \quad q \equiv \frac{Q_D}{A_\Sigma}, \quad (3.26)$$

which may be interpreted as the mass and charge per unit area.

On the other hand, from the above derivation of the solutions one can see that they represent the most general solutions of the Einstein-Maxwell field equations coupled with the cosmological constant in  $D$ -dimensional spacetimes described by the metric (3.2). In general the spacetime is singular at  $r = 0$  and all the other singularities are coordinate ones. This can be seen, for example, from the Ricci scalar, which now is given by

$${}^{(D)}R = -\frac{(D-3)(D-4)Q^2}{r^{2(D-2)}} + \frac{2D}{D-2}\Lambda_D. \quad (3.27)$$

Thus, to have a geodesically complete spacetime one needs to extend the spacetime beyond these coordinate singularities. In the next section, we shall restrict ourselves only to the case where  $k_D = 0$  and  $D = 4$ .

#### IV. FLAT TOPOLOGICAL BLACK HOLES IN FOUR-DIMENSIONAL SPACETIMES

To study the global structure of the solutions given in the above section, in this section we shall restrict ourselves only to the flat case,  $k_D = 0$ , and assume that the spacetime has only four-dimensions,  $D = 4$ . Then, the surface of constant  $t$  and  $r$  can be a plane, a cylinder, a Möbius band, a torus, or a Klein bottle, depending on how to identify the two coordinates in  $X^2$  [13].

Setting  $k = 0$  and  $D = 4$  in Eq.(3.21) we find that the corresponding metric can be written in the form,

$$ds^2 = -f(x)dt^2 + f^{-1}(x)dx^2 + x^2(dy^2 + dz^2), \quad (4.1)$$

where

$$\begin{aligned} f(x) &= \frac{2b}{x} + \frac{q^2}{x^2} - \frac{\Lambda}{3}x^2, \\ F_{\mu\nu} &= \frac{q}{x^2}(\delta_\mu^0\delta_\nu^1 - \delta_\mu^1\delta_\nu^0), \end{aligned} \quad (4.2)$$

with  $b \equiv -M$ ,  $q \equiv Q$  and  $\Lambda$  actually being  $\Lambda_D$ . To consider the most general case, we assume that the mass parameter  $b$  and the coordinate  $x$  take their values from the range  $-\infty < b, x < +\infty$ . It is interesting to note that if we make the replacement  $(M, r) \rightarrow (-M, -r)$ , we find that the Reissner-Nordström solution coupled with a cosmological constant remains the same. That is, the physics for  $M \geq 0$ ,  $r \geq 0$  is the same as that for  $M \leq 0$ ,  $r \leq 0$ . When the spacetime has plane symmetry, the range of the coordinate  $x$  is  $-\infty < x < +\infty$ . This is the main reason why here we are allowed ourselves also to consider the case where  $b > 0$ .

It should be noted that the above solutions was also studied [5]. Since here we would like to give a systematical study for this case, some of the materials to be presented below will be unavoidably overlapped with some presented there.

From Eq.(4.1) we can see that the metric is singular on the hypersurfaces  $f(x) = 0$ . However, these singularities are coordinate singularities, except for the one located on the hypersurface  $x = 0$ . This can be seen, for example, from Eq.(3.27) as well as the corresponding Kretschmann scalar, which now is given by

$$\mathcal{R} \equiv R^{\mu\nu\lambda\delta}R_{\mu\nu\lambda\delta} = 8 \left\{ \frac{1}{x^8} \left[ 6(q^2 + bx)^2 + q^4 \right] + \frac{1}{3}\Lambda^2 \right\}. \quad (4.3)$$

The above expression shows clearly that the Kretschmann scalar becomes unbounded only when  $x \rightarrow 0$ . As  $|x| \rightarrow +\infty$  the spacetime is asymptotically de Sitter or anti-de Sitter, depending on the signs of the cosmological constant,  $\Lambda$ . Thus, only the singularity at  $x = 0$  is a spacetime curvature singularity, which divides the whole  $(t, x)$ -plane into two causally disconnected regions,  $x > 0$  and  $x < 0$ . All the other singularities are coordinate ones, and to have a geodesically complete spacetime, we need to extend the metric beyond these singularities.

In the stationary axisymmetric case, a significant quantity that characterizes a horizon is the surface gravity [14]. In the following we shall derive this quantity for the spacetimes described by the metric (4.1) [15]. To this end, let us consider the four-acceleration of a static observer with the four-velocity  $u^\mu = f^{-1/2}\delta_t^\mu$ ,

$$a^\mu \equiv u^\mu{}_{;\nu}u^\nu = \kappa(x)\delta_x^\mu, \quad (4.4)$$

where

$$\kappa(x) \equiv \frac{1}{2}f_{,x}(x). \quad (4.5)$$

From the above equations we can see that in order to stay at a fixed point  $x$ , the observer has to fire a jet engine whose thrust per unit mass is  $|\kappa(x)|$  in the positive  $x$ -direction for  $f_{,x}(x) > 0$ , and negative  $x$ -direction for  $f_{,x}(x) < 0$ . On the horizon  $x = x_0$ , where  $f(x_0) = 0$ , the quantity  $\kappa$  defined by

$$\kappa \equiv \kappa(x_0) = \frac{1}{2}f_{,x}(x_0), \quad (4.6)$$

is called the surface gravity of the horizon <sup>1</sup>.

---

<sup>1</sup>Note the similarity to the spherical case:  $ds^2 = f(r)dt^2 - f(r)^{-1}dr^2 - r^2(d\theta^2 + \sin^2\theta d\phi^2)$ . For a static observer with the four-velocity  $u^\mu = f^{-1/2}\delta_t^\mu$ , its four-acceleration is given by  $a^\mu = u^\mu{}_{;\nu}u^\nu = (f_{,r}/2)\delta_r^\mu$ . The quantity  $\kappa \equiv f_{,r}(r_g)/2$  is called the surface gravity of the horizon at  $r = r_g$  [14].

To extend the spacetime across the horizon, we can first introduce a new coordinate  $x^*$  by [16]

$$x^* = \int \frac{dx}{f(x)}, \quad (4.7)$$

and then two null coordinates,  $v$  and  $w$ , via the relations

$$v = e^{\kappa(t+x^*)}, \quad w = -e^{-\kappa(t-x^*)}. \quad (4.8)$$

In terms of  $v$  and  $w$ , metric (4.1) becomes

$$ds^2 = -\kappa^{-2}f(x)e^{-2\kappa x^*} dv dw + x^2(dy^2 + dz^2). \quad (4.9)$$

To study the global structure of the spacetime, it is found convenient to distinguish the following cases:

$$\begin{aligned} A) & b \neq 0, q \neq 0, \Lambda = 0; & B) & b \neq 0, q = 0, \Lambda \neq 0; \\ C) & b = 0, q \neq 0, \Lambda \neq 0; & D) & b \neq 0, q \neq 0, \Lambda \neq 0; \\ E) & b \neq 0, q = 0, \Lambda = 0; & F) & b = 0, q \neq 0, \Lambda = 0; \\ G) & b = 0, q = 0, \Lambda \neq 0. \end{aligned} \quad (4.10)$$

In the above classification, Case E) corresponds to the Taub vacuum solution [17] and the properties of which are well-known. In particular, it has a naked singularity at  $x = 0$ . Case F) represents a pure electromagnetic field with a naked singularity at  $x = 0$ , while Case G) corresponds to the de Sitter or anti-de Sitter spacetime, depending on the sign of the cosmological constant. The global structure of the latter is studied extensively in [18]. Therefore, in the following we shall focus our attention only on the first four cases.

#### A. $b \neq 0, q \neq 0, \Lambda = 0$ .

When  $\Lambda = 0$ , we find

$$\begin{aligned} f(x) &= \frac{2b}{x^2} \left( x + \frac{q^2}{2b} \right), \\ f'(x) &= -\frac{2b}{x^3} \left( x + \frac{q^2}{b} \right). \end{aligned} \quad (4.11)$$

Now let us consider the two cases  $b < 0$  and  $b > 0$  separately.

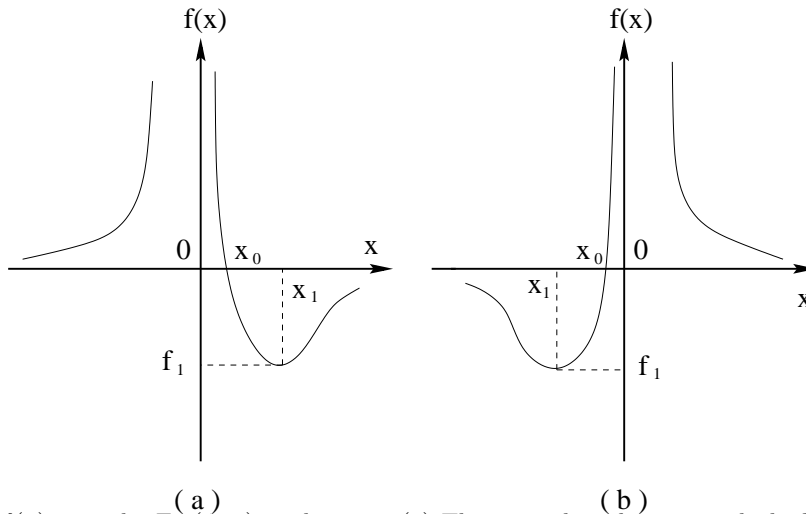


FIG. 1. The function  $f(x)$  given by Eq.(4.11) in the text. (a) The case where  $b < 0$ , in which the function  $f(x)$  is zero at  $x = x_0 \equiv q^2/(2|b|)$  and has a minimum at  $x = x_1 \equiv 2x_0$ , where  $f_1(x_1) = -b^2/q^2$ . (b) The function  $f(x)$  for  $b > 0$  and now we have  $x_0 \equiv -q^2/(2b) < 0$  and  $f_1(2x_0) = -b^2/q^2$ .

**Case A.1)**  $b < 0$ : In this case the function  $f(x)$  is positive in the whole region  $x < 0$  [cf. Fig. 1(a)], and the singularity at  $x = 0$  is naked. The corresponding Penrose diagram is that of Fig. 2. Note that now  $\kappa(x) = f'(x)/2 = (|bx| + q^2)|x|^{-3}$  is also positive in this region, so the naked singularity at  $x = 0$  produces a repulsive force to a stationary observer who stays in this region. Consequently, the naked singularity should effectively have negative gravitational mass.

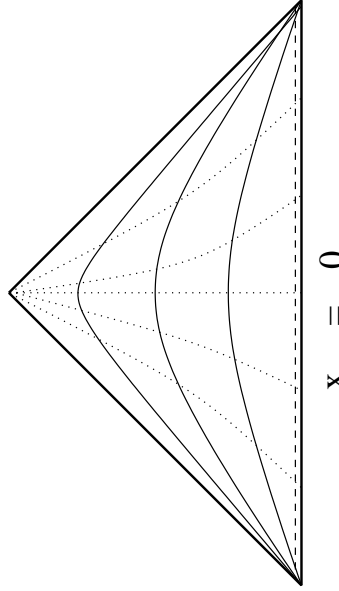


FIG. 2. The Penrose diagram for the solution of Eq.(4.11) with  $b < 0$  in the region  $x < 0$ . The singularity at  $x = 0$  is timelike and naked. The vertical curves are the hypersurfaces  $x = \text{Const.}$  and the horizontal dotted lines are the ones  $t = \text{Const.}$

However, in the region  $x > 0$ , the function  $f(x)$  becomes zero at the point

$$x_0 = \frac{q^2}{2|b|} > 0, \quad (b < 0), \quad (4.12)$$

and the corresponding surface gravity is given by

$$\kappa = -\frac{4|b|^3}{q^4}, \quad (b < 0). \quad (4.13)$$

Thus, a stationary observer near the hypersurface  $x = x_0$  in this region feels a repulsive force from the region  $0 < x < x_0$ , and the totally effective gravitational mass should be also negative in this region. Integrating Eq.(4.7) we obtain

$$x^* = \frac{x^2}{4b} - \frac{q^2 x}{4b^2} + \frac{q^4}{8b^3} \ln(q^2 - 2|b|x). \quad (4.14)$$

On the other hand, the coefficient  $g_{vw}$  now is given by

$$g_{vw} = -(\sqrt{2}\kappa x)^{-2} \exp\left(-\frac{2|b|x}{q^4}(q^2 + |b|x)\right), \quad (4.15)$$

which shows that the metric now is well defined across the hypersurface  $x = x_0$ . Combining Eqs.(4.8) and (4.14), we also have

$$vw = -(q^2 - 2|b|x) \exp\left(\frac{2|b|^2}{q^4}x^2 + \frac{2|b|}{q^2}x\right), \quad (4.16)$$

$$v = (q^2 - 2|b|x)^{1/2} \exp\left(-\frac{4|b|^3}{q^4}t + \frac{|b|^2}{q^4}x^2 + \frac{|b|}{q^2}x\right) \quad (\text{Region I}). \quad (4.17)$$

From the above expressions we can see that the coordinate transformations (4.8) are restricted only to the region where  $v > 0$  and  $w < 0$ , which will be referred to as region  $I$  [cf. Fig. 3]. To extend the metric (4.9) to cover the whole spacetime, one simply takes the range of  $v$  and  $w$  as  $-\infty < v, w < +\infty$ . Then, in the  $(v, w)$ -coordinates we obtain three extended regions  $I', II$  and  $II'$ , which are absent in the  $(t, x)$ -coordinates. In each of the three extended regions, the coordinate transformations from  $(v, w)$  to  $(t, x)$  are given by

$$\begin{aligned} v &= -(q^2 - 2|b|x)^{1/2} \exp\left(-\frac{4|b|^3}{q^4}t + \frac{|b|^2}{q^4}x^2 + \frac{|b|}{q^2}x\right), \quad (\text{Region } I'), \\ v &= (2|b|x - q^2)^{1/2} \exp\left(-\frac{4|b|^3}{q^4}t + \frac{|b|^2}{q^4}x^2 + \frac{|b|}{q^2}x\right), \quad (\text{Region } II), \\ v &= -(2|b|x - q^2)^{1/2} \exp\left(-\frac{4|b|^3}{q^4}t + \frac{|b|^2}{q^4}x^2 + \frac{|b|}{q^2}x\right), \quad (\text{Region } II'), \end{aligned} \quad (4.18)$$

where  $w$  can be found through Eq.(4.16). Then, the corresponding Penrose diagram is that of Fig. 3. From there we can see that the hypersurfaces  $x = x_0$  (or  $vw = 0$ ) are Cauchy horizons that separate the two regions  $I$  and  $I'$  from the two asymptotically flat (only in the  $x$ -direction) ones  $II$  and  $II'$  [18]. The time-like coordinate  $t$  is past-directed in region  $I$  and future-directed in region  $I'$ , as we can see from Eqs.(4.16)-(4.18). Across the horizons,  $t$  becomes space-like, while  $x$  becomes time-like.

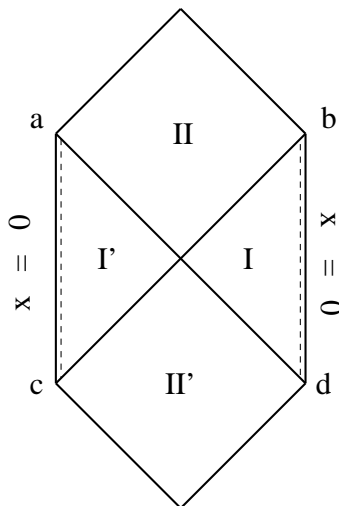


FIG. 3. The Penrose diagram for the solution of Eq.(4.11) with  $b < 0$  in the region  $x > 0$ . The singularity at  $x = 0$  is timelike and the lines  $bc$  and  $ad$  where  $x = x_0$  are Cauchy horizons.

**Case A.2)**  $b > 0$ : In this case the spacetime properties can be obtained from the case  $b < 0$  by the replacement  $(b, x) \rightarrow (-b, -x)$ . In particular, in the region  $x > 0$  the function  $f(x)$  is strictly positive and the singularity at  $x = 0$  is naked. The corresponding Penrose diagram is similar to that given by Fig. 2, but now with  $x > 0$ . In the region  $x < 0$ , the metric becomes singular at the hypersurface  $x = x_0 \equiv -q^2/(2b)$  [cf. Fig. 1(b)], on which we now have

$$\kappa = \frac{4b^3}{q^4} > 0, \quad (b > 0). \quad (4.19)$$

That is, a stationary observer near the hypersurface  $x = x_0$  in this region feels a repulsive force from the region  $x_0 < x < 0$ . After extending the spacetime beyond this surface, the corresponding Penrose diagram is similar to that of Fig. 3 but with  $x < 0$ .

#### B. $b \neq 0, q = 0, \Lambda \neq 0$ .

When  $q = 0$ , we have

$$f(x) = \frac{\Lambda}{3x} \left( \frac{6b}{\Lambda} - x^3 \right). \quad (4.20)$$



In this case it is found convenient to distinguish the four subcases,

$$\begin{aligned} 1) \Lambda > 0, \quad b > 0; \quad 2) \Lambda > 0, \quad b < 0; \\ 3) \Lambda < 0, \quad b < 0; \quad 4) \Lambda < 0, \quad b > 0. \end{aligned} \tag{4.21}$$

**Case B.1)**  $\Lambda > 0, b > 0$ : In this subcase, we find that  $f(x)$  is negative for all  $x < 0$ . Thus, in this region  $x$  is timelike and  $t$  is spacelike. Then, the singularity at  $x = 0$  is spacelike and naked. So, in this region the spacetime has a global structure that is quite similar to some cosmological models.

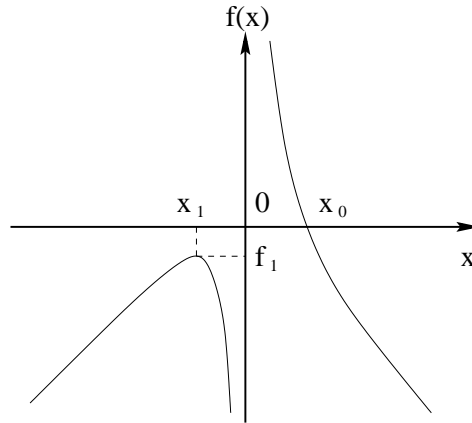


FIG. 4. The function  $f(x)$  given by Eq.(4.20) in the text, where  $x_1 \equiv -(3b/\Lambda)^{1/3}$  and  $f_1(x_1) = -[(3b)^2\Lambda]^{1/3} < 0$ .

In the region  $x > 0$  the function  $f(x)$  is positive only for  $0 \leq x \leq x_0$  [cf. Fig. 4], where

$$x_0 = \left(\frac{6b}{\Lambda}\right)^{1/3}. \tag{4.22}$$

On the hypersurface  $x = x_0$  we have  $f(x_0) = 0$ , which, as shown before, is only a coordinate singularity. Thus, we need to extend the solution beyond this hypersurface. Before doing so, we first note that now we have

$$\kappa = -\frac{\Lambda}{2}x_0 < 0, \tag{4.23}$$

that is, an observer near the horizon will feel a repulsive force from the region  $0 < x < x_0$ . Then, we would expect that the singularity at  $x = 0$  has an effectively negative gravitational mass. This is understandable, since in the present case we have  $\Lambda > 0$ , which is energetically equivalent to a matter field with a negative mass density.

Following the same line as outlined in the last subcase, we find that the corresponding Penrose diagram is given by Fig. 5. The hypersurfaces  $x = x_0$  (or  $vw = 0$ ) are Cauchy horizons. The singularities at  $x = 0$  now are also timelike. The coordinate  $t$  is past-directed in region  $I$  and future-directed in region  $I'$ .

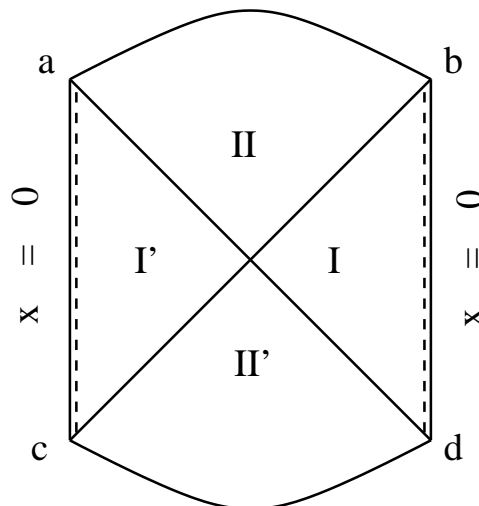


FIG. 5. The Penrose diagram for the solution of Eq.(4.20) with  $b > 0$  and  $\Lambda > 0$  in the region  $x > 0$ . The singularity at  $x = 0$  is timelike and the lines  $bc$  and  $ad$  where  $x = x_0$  are Cauchy horizons. On the curved lines  $ab$  and  $cd$  we have  $x = \infty$ .

**Case B.2)**  $\Lambda > 0, b < 0$ : From Eq.(4.20) we can see that this case can be obtained from the last case by the replacement  $(x, b) \rightarrow (-x, -b)$ . Thus, the spacetime structure for this case can be also obtained from the ones given in the last case by this replacement. In particular, now the solution in the region  $x > 0$  may represent a cosmological model, and the spacetime has a naked singularity at  $x = 0$ , which is spacelike. In the region  $x < 0$ , the corresponding Penrose diagram is that of Fig. 5 but now with  $x < 0$ .

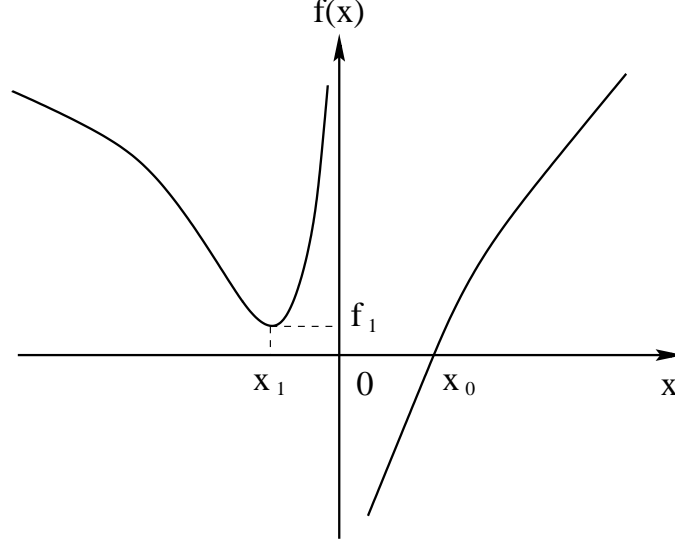


FIG. 6. The function  $f(x)$  given by Eq.(4.24) in the text, for  $\Lambda < 0$  and  $b < 0$ , where  $f_1(x_1) = [(3b)^2|\Lambda|]^{1/3} > 0$ .

**Case B.3)**  $\Lambda < 0, b < 0$ : In this case, we find that

$$\begin{aligned} f(x) &= \frac{|\Lambda|}{3x} \left( x^3 - \left| \frac{6b}{\Lambda} \right| \right), \\ f'(x) &= \frac{|2\Lambda|}{3x^2} \left( x^3 + \left| \frac{3b}{\Lambda} \right| \right). \end{aligned} \quad (4.24)$$

Thus, in the region  $x < 0$  the function is always positive as shown by Fig. 6. As a result, the singularity at  $x = 0$  is naked. On the other hand, for any hypersurface  $x = C$ , its normal vector  $n_\alpha$  is given by  $n_\alpha = \partial(x - C)/\partial x^\alpha = \delta_\mu^x$ . Thus, we have

$$x_\alpha x^\alpha = f(x) \rightarrow +\infty, \quad (4.25)$$

as  $x \rightarrow -\infty$ , which means that the spatial infinity  $x = -\infty$  in the present case is timelike. Then, the corresponding Penrose diagram is given by Fig. 7.

It is also interesting to note that now the acceleration of a static observer is given by Eq.(4.4) with

$$\kappa(x) = \frac{|\Lambda|}{3x^2} \left( x^3 + \left| \frac{3b}{\Lambda} \right| \right) = \begin{cases} < 0, & x < x_1, \\ = 0, & x = x_1, \\ > 0, & x_1 < x < 0, \end{cases} \quad (4.26)$$

where  $x_1 \equiv -|3b/\Lambda|^{1/3}$ .

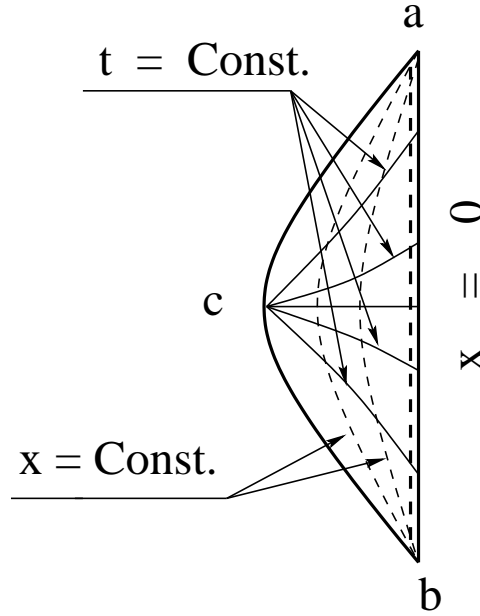


FIG. 7. The Penrose diagram for the solutions given by Eq.(4.24) in the region  $x < 0$  for  $\Lambda < 0$  and  $b < 0$ .

In the region  $x > 0$ , we have

$$f(x) = \begin{cases} < 0, & x < x_0, \\ = 0, & x = x_0, \\ > 0, & x > x_0, \end{cases} \quad (4.27)$$

where  $x_0 \equiv |6b/\Lambda|^{1/3}$ , and

$$\kappa \equiv \frac{1}{2}f'(x_0) = \left| \frac{\Lambda}{2} \right| x_0 > 0. \quad (4.28)$$

Extending the solutions into the region  $0 < x < x_0$ , we find the following relevant quantities

$$g_{vw} = -\frac{2(x^2 + x_0x + x_0^2)^{3/2}}{3|\Lambda|x_0^2x} \exp \left\{ -\sqrt{3} \operatorname{arctg} \left( \frac{2x + x_0}{\sqrt{3}x_0} \right) \right\},$$

$$vw = -\frac{x - x_0}{(x^2 + x_0x + x_0^2)^{1/2}} \exp \left\{ \sqrt{3} \operatorname{arctg} \left( \frac{2x + x_0}{\sqrt{3}x_0} \right) \right\}, \quad (4.29)$$

$$v = \frac{(x - x_0)^{1/2}}{(x^2 + x_0x + x_0^2)^{1/4}} \exp \left\{ -\frac{\Lambda}{2}x_0t + \frac{\sqrt{3}}{2} \operatorname{arctg} \left( \frac{2x + x_0}{\sqrt{3}x_0} \right) \right\} \quad (\text{Region } I). \quad (4.30)$$

The corresponding Penrose diagram is given by Fig. 8, which shows that now the hypersurfaces  $x = x_0$  (or  $vw = 0$ ) represent event horizons, and the singularities at  $x = 0$  are space-like. Regions  $II$  and  $III'$  are two catastrophic regions, while regions  $I$  and  $I'$  are two asymptotically anti-de Sitter regions. The time-like coordinates  $t$  is future-directed in region  $I$  and past-directed in region  $I'$ . Region  $II$  can be considered as a black hole, while region  $III'$  as a white hole. Since now the surface gravity of the horizon is positive, the spacetime singularity at  $x = 0$  is gravitationally attractive and expected to have an effectively positive gravitational mass.

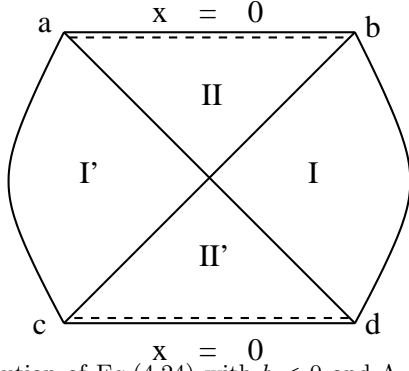


FIG. 8. The Penrose diagram for the solution of Eq.(4.24) with  $b < 0$  and  $\Lambda < 0$  in the region  $x > 0$ . The singularity at  $x = 0$  is spacelike and the lines  $bc$  and  $ad$  where  $x = x_0$  represent event horizons, while the curved lines  $ac$  and  $bd$  represent the spatial infinity  $x = \infty$ .

**Case B.4)**  $\Lambda < 0, b > 0$ : This is the case which corresponds to Case B.3). As a matter of fact, replacing  $x$  by  $-x$ , we can obtain one from the other. Therefore, the corresponding Penrose diagrams in the two subcases are the same, after the above replacement is taken into account.

**C.**  $b = 0, q \neq 0, \Lambda \neq 0$ .

When  $b = 0$ , from Eq.(4.2) we can see that  $f(x) = f(-x)$ . Thus, the spacetime has reflection symmetry with respect to the hypersurface  $x = 0$ . Then, without loss of generality, in the following we shall only consider the region  $x > 0$  in this case.

When  $\Lambda < 0$ ,  $f(x)$  is always greater than zero for any  $x$ . Consequently, the singularity at  $x = 0$  is naked, and the corresponding Penrose diagram is similar to that of Fig. 7.

When  $\Lambda > 0$ , we have

$$f(x) = \frac{\Lambda}{3x^2}(x_0^2 + x^2)(x_0^2 - x^2), \quad (4.31)$$

but now  $x_0$  is given by

$$x_0 \equiv \left(\frac{3q^2}{\Lambda}\right)^{1/4}. \quad (4.32)$$

From the above equations we can see that  $f(x) \geq 0$  holds only in the region  $0 < x < x_0$ . On the hypersurface  $x = x_0$  the surface gravity is given by

$$\kappa = -\frac{2\Lambda}{3}x_0 < 0, \quad (4.33)$$

that is, the effective gravitational mass in the region  $0 < x < x_0$  should be negative. One can show that the corresponding Penrose diagram is similar to that of Fig. 5.

**D.**  $b \neq 0, q \neq 0, \Lambda \neq 0$ .

When none of the three parameters are zero, we need to distinguish the four subcases as defined by Eq.(4.21). However, as shown in Cases A) and B), the properties of the spacetimes for the case  $b < 0$  can be obtained from those for the case  $b > 0$  by simply replacing  $x$  by  $-x$ . Thus, we actually need to consider only the subcases  $\Lambda > 0, b > 0$ , and  $\Lambda < 0, b < 0$ .

**Case D.1)**  $\Lambda > 0, b > 0$ : In this case, it can be shown that  $f(x)$  takes the form

$$f(x) = \frac{\Lambda}{3x^2}(x_+ - x)(x - x_-)(x^2 + Bx + C), \quad (4.34)$$

where

$$B \equiv x_+ + x_-, \quad C \equiv x_+^2 + x_+x_- + x_-^2, \quad (4.35)$$

and  $x_{\pm}$  are the two real roots of the equation  $f(x) = 0$ , given via the relations

$$B(x_+^2 + x_-^2) = \frac{6b}{\Lambda}, \quad Cx_+x_- = -\frac{3q^2}{\Lambda}, \quad (4.36)$$

with the property

$$x_+ > 0, \quad x_- < 0. \quad (4.37)$$

From the above equations we can see that  $f(x) \geq 0$  is true only in the region  $x_- \leq x < 0$  or  $0 < x \leq x_+$ . Then, we need to extend the solutions beyond both of the hypersurfaces  $x = x_{\pm}$ .

Let us first consider the extension across the hypersurface  $x = x_+$ . We first note that

$$\kappa|_{x=x_+} = -\frac{\Lambda}{6x_+^2}(x_+ - x_-)(x_+^2 + Bx_+ + C) < 0. \quad (4.38)$$

Thus, a static observer near the horizon will feel a repulsive force from the region  $0 < x < x_+$ , which means that the effective gravitational mass in this region is negative. One can also show that the Penrose diagram is similar to that given by Fig. 5.

On the other hand, the surface gravity at  $x = x_-$  is given by

$$\kappa|_{x=x_-} = \frac{\Lambda}{6x_-^2}(x_+ - x_-)(x_-^2 + Bx_- + C) > 0, \quad (4.39)$$

which means, similar to that in the region  $x > 0$ , now a static observer near the horizon will also feel a repulsive force from the region  $x_- < x < 0$ . It can be also shown that the corresponding Penrose diagram is that of Fig. 5, but with  $x < 0$ .

**Case D.2)**  $\Lambda < 0, b < 0$ : In this case we find that it is convenient to distinguish the following three subcases:

$$i) |q| < q_c, \quad ii) |q| = q_c, \quad iii) |q| > q_c, \quad (4.40)$$

where

$$q_c \equiv |\Lambda|^{-1/6} \left| \frac{3b}{2} \right|^{2/3}. \quad (4.41)$$

**Case D.2.i)**  $|q| < q_c$ : In this case, it is found that the function  $f(x)$  can be written as

$$f(x) = \frac{|\Lambda|}{3x^2}(x - x_+)(x - x_-)(x^2 + Bx + C), \quad (4.42)$$

where  $B, C$  and  $x_{\pm}$  are given by Eqs.(4.35) and (4.36), but now with the properties

$$x_+ > 0, \quad x_- > 0, \quad (|q| < q_c). \quad (4.43)$$

From Eqs.(4.42) and (4.43) we can see that in the region  $x < 0$  the function  $f(x)$  is positive, and the singularity at  $x = 0$  is naked [cf. Fig. 9]. The corresponding Penrose diagram is similar to that given by Fig. 7.

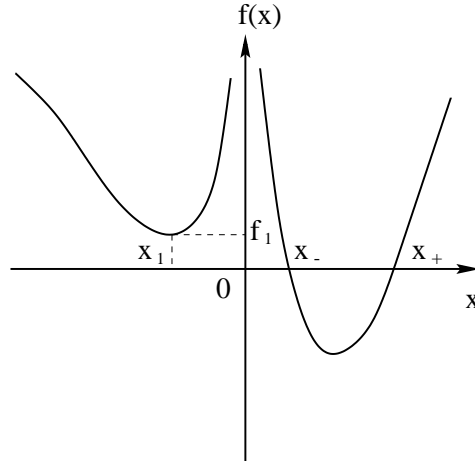


FIG. 9. The function  $f(x)$  given by Eq.(4.42) in the text, for  $\Lambda < 0$ ,  $b < 0$  and  $|q| < q_c$ , where  $f_1(x_1) = [(3b)^2|\Lambda|]^{1/3} > 0$ .

When  $x > 0$ ,  $f(x)$  is non-negative only in the regions  $x \geq x_+$  or  $0 \leq x \leq x_-$ . Thus, an extension across the hypersurfaces  $x = x_{\pm}$  is needed. Let us first consider the extension across  $x = x_+$ .

**The extension across the hypersurface  $x = x_+$ :** Following previous cases, we find the following,

$$\begin{aligned}
x^* &= \frac{1}{2\kappa_+} \ln(x - x_+) + \sum_{n=1}^{\infty} \frac{a_n}{n} (x - x_+)^n, \\
\kappa_+ &= \frac{f_{,x}(x_+)}{2} = \frac{|\Lambda|}{6x_+^2} (x_+ - x_-)(x_+^2 + bx_+ + c) > 0, \\
f(x) &= \frac{x - x_+}{g(x)}, \quad a_n = \frac{1}{n!} \left. \frac{d^n g(x)}{dx^n} \right|_{x=x_+}, \\
g_{vw} &= -[2\kappa_+^2 g(x)]^{-1} \exp \left\{ -2\kappa_+ \sum_{n=1}^{\infty} \frac{a_n}{n} (x - x_+)^n \right\}, \\
vw &= -(x - x_+) \exp \left\{ 2\kappa_+ \sum_{n=1}^{\infty} \frac{a_n}{n} (x - x_+)^n \right\}, \\
v &= (x - x_+)^{1/2} \exp \left\{ \kappa_+ \left[ t + \sum_{n=1}^{\infty} \frac{a_n}{n} (x - x_+)^n \right] \right\}, \quad (\text{Region } I).
\end{aligned} \tag{4.44}$$

Then, we get four regions,  $I$ ,  $I'$ ,  $II$  and  $II'$  in the  $(v, w)$ -plane, as shown in Fig. 10. The hypersurfaces  $x = x_+$  now are event horizons. The coordinate  $t$  is future-directed in region  $I$  and past-directed in region  $I'$ . Note that as  $x \rightarrow +\infty$ , we have  $f(x) \rightarrow +\infty$ . Therefore, the hypersurface  $x = +\infty$  is timelike and represented by the curves  $ac$  and  $bd$  in Fig. 10.

**The extension across the hypersurface  $x = x_-$ :** Now we find that

$$\begin{aligned}
x^* &= \frac{1}{2\kappa_-} \ln(x - x_-) + \sum_{n=1}^{\infty} \frac{b_n}{n} (x - x_-)^n, \\
\kappa_- &= \frac{f_{,x}(x_-)}{2} = -\frac{|\Lambda|}{6x_-^2} (x_+ - x_-)(x_-^2 + bx_- + c) < 0, \\
f(x) &= \frac{x - x_-}{\bar{g}(x)}, \quad b_n = \frac{1}{n!} \left. \frac{d^n \bar{g}(x)}{dx^n} \right|_{x=x_-}, \\
g_{vw} &= -[2\kappa_-^2 \bar{g}(x)]^{-1} \exp \left\{ -2\kappa_- \sum_{n=1}^{\infty} \frac{b_n}{n} (x - x_-)^n \right\}, \\
vw &= -(x - x_-) \exp \left\{ -2\kappa_- \sum_{n=1}^{\infty} \frac{b_n}{n} (x - x_-)^n \right\}, \\
v &= (x - x_-)^{1/2} \exp \left\{ \kappa_- \left[ t + \sum_{n=1}^{\infty} \frac{b_n}{n} (x - x_-)^n \right] \right\}, \quad (\text{Region } III).
\end{aligned} \tag{4.45}$$

Clearly, by this extension, we get two more regions  $III$  and  $III'$ , as shown in Fig. 10. The singularities at  $x = 0$  are time-like and repulsive, since now we have  $\kappa_- < 0$ . The hypersurfaces  $x = x_-$  represent Cauchy horizons. Extensions across these hypersurfaces are further needed in order to have a geodesically complete spacetime. However, since these surfaces are Cauchy horizons, the extensions across them are not unique, a situation quite similar to that of the Reissner-Nordstrom (RN) or Kerr solution [18].

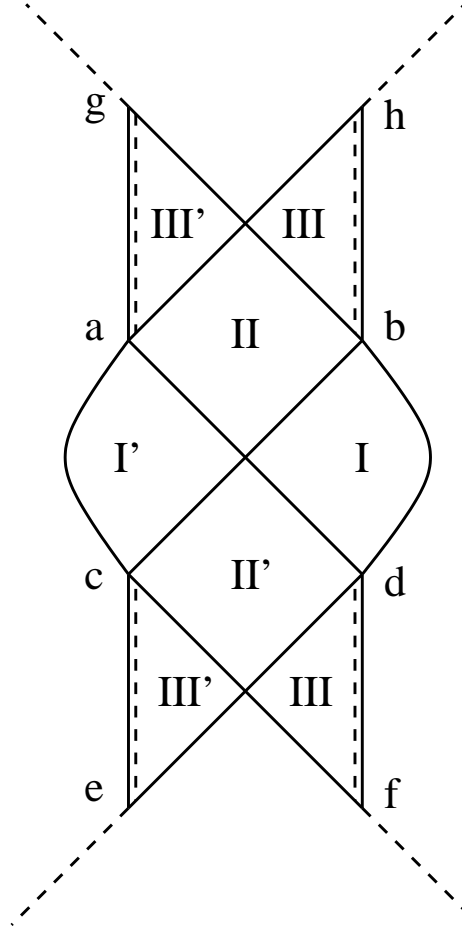


FIG. 10. The Penrose diagram for the solution of Eq.(4.42) with  $|q| < q_c$  in the region  $x > 0$ . The lines  $ad$  and  $bc$  where  $x = x_+$  represent event horizons, and the ones  $gb$ ,  $ha$ ,  $cf$  and  $de$ , where  $x = x_-$ , represent Cauchy horizons. The singularities at  $hb$ ,  $ga$ ,  $df$  and  $ce$  are timelike. The curves  $ac$  and  $bd$  represent the spatial infinity ( $x = \infty$ ), which is timelike. To have a geodesically maximal spacetime, the extension in the vertical directions should be continuous to infinity.

**Case D.2.ii)**  $|q| = q_c$ : In this case, we find

$$f(x) = \frac{|\Lambda|}{3x^2}(x - x_0)^2(x^2 + 2x_0x + 3x_0^2), \quad (4.46)$$

where  $x_0$  now is given by

$$x_0 = \left(\frac{3b}{2\Lambda}\right)^{1/3}. \quad (4.47)$$

Thus,  $f(x) > 0$  holds for all  $x < 0$ . As a result, in the region  $x < 0$  the singularity at  $x = 0$  is naked, and the corresponding Penrose diagram is that of Fig. 7.

In the region  $x > 0$ ,  $f(x)$  is also positive, except at the point  $x = x_0$ , where  $f(x_0) = 0$ . See Fig. 9, and notice that now we have  $x_+ = x_- = x_0$ . This is quite similar to the extreme case of the RN solution [18]. Integrating Eq.(4.7), we obtain

$$\begin{aligned} x^* = & -\frac{x}{2|\Lambda|x_0(x - x_0)} + \frac{1}{3|\Lambda|x_0} \ln \frac{(x - x_0)^2}{x^2 + 2x_0x + 3x_0^2} \\ & + \frac{7\sqrt{2}}{12|\Lambda|x_0} \operatorname{arctg} \left( \frac{x + x_0}{\sqrt{2}x_0} \right) + x_0^*, \end{aligned} \quad (4.48)$$

where  $x_0^*$  is an integration constant. In the following, without loss of generality, we shall choose  $x_0^*$  such that  $x^*(0) = 0$ . On the other hand, from Eqs.(4.6) and (4.46) we find

$$\kappa = \frac{1}{2}f_{,x}(x_0) = 0. \quad (4.49)$$

That is, the surface gravity now is zero. As a result, the usual method of the extension given by Eqs.(4.7)-(4.9) is not applicable to this case, and we have to consider other possibilities. Following Carter [19], let us define the two null coordinates  $v$  and  $w$  by

$$v = \tan^{-1}(t + x^*), \quad w = \tan^{-1}(t - x^*), \quad (4.50)$$

where  $-\pi/2 \leq v \leq 3\pi/2$ , and  $-3\pi/2 \leq w \leq \pi/2$ . In terms of  $v$  and  $w$ , the metric reads

$$ds^2 = -\frac{f(x)}{\cos^2 v \cos^2 w} dv dw + x^2(dy^2 + dz^2). \quad (4.51)$$

Using the relation

$$\frac{\sin^2(v - w)}{\cos^2 v \cos^2 w} = 4(x^*)^2, \quad (4.52)$$

one can show that the metric coefficients of Eq.(4.51) become regular across the hypersurface  $x = x_0$ . Thus, it represents an extension. As a matter of fact, one can show that this extension is analytic and the extended spacetime is given by regions  $I$  and  $III$  in Fig. 11, which is quite similar to the extreme RN black hole [18]. The only difference is that in the present case the hypersurface  $x = +\infty$  is time-like, since as  $x \rightarrow +\infty$  we now have  $x^* \rightarrow \text{finite}$ . Keeping this in mind, we can deduce all the properties of this solution from the extreme RN black hole. For example, the horizons  $x = x_0$  represent event horizons. The region  $x_0 < x < +\infty$  is mapped to region  $I$ , while the one  $0 < x < x_0$  to region  $III$ . The  $t$ -coordinate is future-directed in region  $I$ . The singularity at  $x = 0$ , represented by the vertical double-lines in Fig. 11, is time-like. From the diagram we can see that the extension should be continuous to infinity in the vertical directions, in order to get a geodesically complete spacetime.

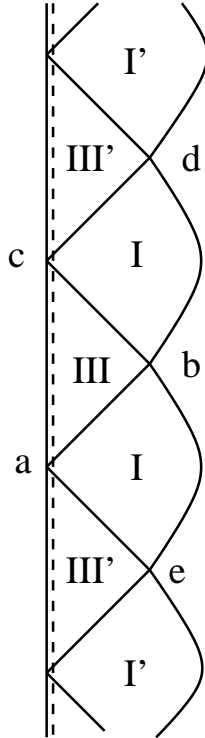


FIG. 11. The Penrose diagram for the solutions given by Eq.(4.46) in the text with  $|q| = q_c$  and in the region  $x > 0$ . The spacetime singularity at  $x = 0$ , represented by the vertical line  $ac$ , is timelike. The surfaces  $ae, ab, cb$ , and  $cd$ , where  $x = x_0$ , all represent event horizons. The hypersurfaces  $x = +\infty$  now are timelike, given by the curves  $bd$  and  $eb$ . The extension in the vertical directions is continuous to infinity.



**Case D.2.iii)**  $|q| > q_c$ : In this case it can be shown that  $f(x) > 0$  holds for any  $x$ . As a result, the singularity at  $x = 0$  is naked, and the corresponding Penrose diagram is given by Fig. 7.

## V. TYPE II FLUID IN D-DIMENSIONAL SPACETIMES

Now using the gauge freedom of Eq.(2.2), we shall set

$$g_{11}(x^c) = 0, \quad s = r, \quad (5.1)$$

where  $x^a = \{v, r\}$ . These coordinates are usually called *Eddington-Finkelstein coordinates*, in terms of which the metric (2.1) takes the form,

$$ds^2 = -e^{\psi(v,r)} dv \left( f(v,r) e^{\psi(v,r)} dv + 2\epsilon dr \right) + r^2 h_{AB}(x^C) dx^A dx^B, \quad (5.2)$$

where  $\epsilon = \pm 1$ . When  $\epsilon = 1$ , the radial coordinate  $r$  increases towards the future along a ray  $v = \text{Const}$ . When  $\epsilon = -1$ , the radial coordinate  $r$  decreases towards the future along a ray  $v = \text{Const}$ .

From Eq.(2.8) it can be shown that

$$\begin{aligned} {}^{(2)}R_{ab} &= \frac{1}{2}A [f e^{\psi} \delta_a^0 \delta_b^0 + \epsilon (\delta_a^0 \delta_b^1 + \delta_a^1 \delta_b^0)], \\ A(v,r) &= e^{\psi} [2f\psi_{,rr} + f_{,rr} + (2f\psi_{,r} + 3f_{,r})\psi_{,r}] - 2\epsilon\psi_{,vr}, \\ \nabla_a \nabla_b r &= -\frac{1}{2}f e^{2\psi} \left( 2f\psi_{,r} + f_{,r} + \epsilon e^{-\psi} \frac{f_{,v}}{f} \right) \delta_a^0 \delta_b^0 \\ &\quad - \frac{1}{2}\epsilon e^{\psi} (2f\psi_{,r} + f_{,r}) (\delta_a^0 \delta_b^1 + \delta_a^1 \delta_b^0) - \psi_{,r} \delta_a^1 \delta_b^1, \\ \square r &= f\psi_{,r} + f_{,r}. \end{aligned} \quad (5.3)$$

Inserting the above expressions into Eq.(2.7), we obtain

$$\begin{aligned} {}^{(D)}R_{vv} &= \frac{1}{2}f e^{2\psi} \left[ 2f\psi_{,rr} + f_{,rr} + (2f\psi_{,r} + 3f_{,r})\psi_{,r} + \frac{D-2}{r} (2f\psi_{,r} + f_{,r}) \right] \\ &\quad - \frac{1}{2}\epsilon f e^{\psi} \left( 2\psi_{,rv} - \frac{(D-2)f_{,v}}{rf} \right), \end{aligned} \quad (5.4)$$

$${}^{(D)}R_{vr} = \frac{1}{2}\epsilon e^{\psi} \left[ 2f\psi_{,rr} + f_{,rr} + (2f\psi_{,r} + 3f_{,r})\psi_{,r} + \frac{D-2}{r} (2f\psi_{,r} + f_{,r}) \right] - \psi_{,rv}, \quad (5.5)$$

$${}^{(D)}R_{rr} = \frac{D-2}{r} \psi_{,r}, \quad (5.6)$$

$${}^{(D)}R_{AB} = [k_D - r(f\psi_{,r} + f_{,r}) - (D-3)f] h_{AB}. \quad (5.7)$$

On the other hand, introducing two null vectors  $l_\mu$  and  $n_\mu$  via the relations

$$\begin{aligned} l_\mu &= \delta_\mu^v, \quad n_\mu = e^{\psi} \left( \frac{1}{2}f e^{\psi} \delta_\mu^v + \epsilon \delta_\mu^r \right), \\ l_\lambda l^\lambda &= 0 = n_\lambda n^\lambda, \quad l_\lambda n^\lambda = -1, \end{aligned} \quad (5.8)$$

we find that the energy-momentum tensor for a Type II fluid can be written as [20,21]

$${}^{(D)}T_{\mu\nu} = \mu l_\mu l_\nu + (\rho + P) (l_\mu n_\nu + l_\nu n_\mu) + P g_{\mu\nu}. \quad (5.9)$$

Then, from the Einstein field equations we find that

$${}^{(D)}R_{\mu\nu} = 8\pi G_D \left\{ \mu l_\mu l_\nu + (\rho + P) (l_\mu n_\nu + l_\nu n_\mu) + \frac{2\rho}{D-2} g_{\mu\nu} \right\}. \quad (5.10)$$

From Eqs.(5.6) and (5.10) we obtain  $\psi_{,r} = 0$ , that is,  $\psi(v,r) = \psi(v)$ . However, by introducing another null coordinate  $\bar{v} = \int e^{\psi(v)} dv$ , we can always set, without loss of the generality,

$$\psi(v, r) = 0, \quad \left( {}^{(D)}G_{rr} = 8\pi G_D {}^{(D)}T_{rr} \right). \quad (5.11)$$

On the other hand, from the rest of the Einstein field equations, we find that

$$\begin{aligned} \mu &= \frac{\epsilon(D-2)}{16\pi G_D r} f_{,v}, \\ \rho &= \frac{D-2}{16\pi G_D r^2} (k_D - r f_{,r} - (D-3)f), \\ P &= \frac{1}{16\pi G_D} \left\{ f_{,rr} + \frac{2(D-3)}{r} f_{,r} - \frac{D-4}{r} [k_D - (D-3)f] \right\}. \end{aligned} \quad (5.12)$$

To see that the energy-momentum tensor given by Eq.(5.9) indeed represents a Type *II* fluid, let us first introduce the following unit vectors,

$$\begin{aligned} E_{(0)}^\mu &= \frac{l^\mu + n^\mu}{\sqrt{2}}, \quad E_{(1)}^\mu = \frac{l^\mu - n^\mu}{\sqrt{2}}, \\ E_{(A)}^\mu &= \frac{1}{r} E_{(A)}^B \delta_B^\mu, \quad g_{\mu\nu} E_{(\alpha)}^\mu E_{(\beta)}^\nu = \eta_{\alpha\beta}, \end{aligned} \quad (5.13)$$

where  $\eta_{\alpha\beta} = \text{diag.}\{-1, 1, 1, \dots, 1\}$ , and  $E_{(A)}^B$  ( $A, B = 2, 3, \dots, D-2$ ) consist of an orthogonal base in the space of  $h_{AB}$ , that is,

$$E_{(A)}^C E_{(B)}^D h_{CD} = \delta_{AB}. \quad (5.14)$$

Then, projecting  $T_{\mu\nu}$  into this base, we find that

$$(T_{(\mu)(\nu)}) = \begin{pmatrix} \frac{1}{2}(\mu + 2\rho) & -\frac{1}{2}\mu & 0 & 0 & \dots & 0 \\ -\frac{1}{2}\mu & \frac{1}{2}(\mu - 2\rho) & 0 & 0 & \dots & 0 \\ 0 & 0 & P & 0 & \dots & 0 \\ 0 & 0 & 0 & P & \dots & 0 \\ \dots & \dots & \dots & \dots & \dots & 0 \\ 0 & 0 & 0 & 0 & \dots & P \end{pmatrix}, \quad (5.15)$$

which is exactly the Type *II* fluid, according to the classification given in [18]. Therefore, for any given function  $f(v, r)$  with  $\psi = 0$ , the corresponding energy-momentum tensor of the metric (5.2) can be always written in the form of a Type *II* fluid. However, not for any choice of  $f(v, r)$  the solution is physically acceptable. In fact, it must satisfy some (geometrical and physical) conditions, such as, the energy conditions [18]. Following [21], we write  $f(v, r)$  in the form

$$\begin{aligned} f(v, r) &= k - \frac{2m(v, r)}{r^{D-3}}, \\ m(v, r) &= \sum_{n=-\infty}^{\infty} a_n(v) r^n. \end{aligned} \quad (5.16)$$

Then, Eq.(5.12) becomes

$$\begin{aligned} \mu &= -\frac{\epsilon(D-2)}{8\pi G_D r^{D-2}} \sum_{n=-\infty}^{\infty} a'_n(v) r^n, \\ \rho &= \frac{D-2}{8\pi G_D r^{D-2}} \sum_{n=-\infty}^{\infty} n a_n(v) r^{n-1}, \\ P &= -\frac{1}{8\pi G_D r^{D-3}} \sum_{n=-\infty}^{\infty} n(n-1) a_n(v) r^{n-2}, \end{aligned} \quad (5.17)$$

where a prime denotes the ordinary differentiation with respect to the indicated argument. Clearly, by properly choosing the coefficients  $a_n(v)$ , we can get many exact solutions. For example, for the choice,

$$a_n(v) = \begin{cases} m(v), & n = 0, \\ -\frac{1}{2}q^2(v), & n = -(D-3), \\ \frac{1}{2}\Lambda, & n = D-1, \\ 0, & \text{otherwise,} \end{cases} \quad (5.18)$$

we find that

$$f(v, r) = k - \frac{2m(v)}{r^{D-3}} + \frac{q^2(v)}{r^{2(D-3)}} - \Lambda r^2, \quad (5.19)$$

and the corresponding energy-momentum tensor can be written as

$${}^{(D)}T_{\mu\nu} = \mu l_\mu l_\nu + {}^{(D)}F_{\mu\alpha} {}^{(D)}F_\nu{}^\alpha - \frac{1}{4} {}^{(D)}F_{\alpha\beta} {}^{(D)}F^{\alpha\beta}, \quad (5.20)$$

with

$$\begin{aligned} {}^{(D)}F_{\mu\nu} &= \left( \frac{(D-2)(D-3)}{2} \right)^{1/2} \frac{q(v)}{r^{D-2}} (\delta_\mu^0 \delta_\nu^1 - \delta_\mu^1 \delta_\nu^0), \\ \mu &= -\frac{\epsilon(D-2)}{8\pi G_D r^{D-2}} \left\{ m'(v) - q(v) \frac{q'(v)}{r^{D-3}} \right\}. \end{aligned} \quad (5.21)$$

When  $k = 1$  and  $D = 4$  the above solutions reduce to the ones found in [21]. Lately, these solutions were generalized to high dimensional spherical spacetimes [22].

## VI. FORMATION OF TOPOLOGICAL BLACK HOLES FROM GRAVITATIONAL COLLAPSE OF A TYPE II FLUID

To consider gravitational collapse of the Type *II* fluid found in the last section let us choose  $\epsilon = -1$ . Then, metric (5.2) with  $\psi = 0$  becomes

$$ds^2 = -f(v, r)dv^2 + 2dvdr + r^2 h_{AB} (x^C) dx^A dx^B. \quad (6.1)$$

To the present purpose, let us consider the solutions given by Eqs.(5.19) - (5.21) with

$$\begin{aligned} m(v) &= \begin{cases} \lambda v_0^{D-3}, & v \geq v_0, \\ \lambda v^{D-3}, & 0 \leq v \leq v_0, \\ 0, & v < 0, \end{cases} \\ q(v) &= \begin{cases} \delta v_0^{D-3}, & v \geq v_0, \\ \delta v^{D-3}, & 0 \leq v \leq v_0, \\ 0, & v < 0, \end{cases} \end{aligned} \quad (6.2)$$

where  $\lambda$  and  $\delta$  are arbitrary real constants, subject to  $\lambda > 0$ . Clearly, the solutions represent a charged null dust fluid moving on a de Sitter or anti-de Sitter background in the region  $0 \leq v \leq v_0$ , depending on the sign of  $\Lambda$ . When  $\Lambda = 0$  the spacetime is self-similar, while when  $\Lambda \neq 0$  it is only asymptotically self-similar,  $(v, r) \rightarrow (0, 0)$ . The corresponding energy-momentum tensor is given by Eq.(5.20) with

$$\begin{aligned} {}^{(D)}F_{\mu\nu} &= \begin{cases} \left( \frac{(D-2)(D-3)}{2} \right)^{1/2} \frac{\delta v_0^{D-3}}{r^{D-2}} (\delta_\mu^0 \delta_\nu^1 - \delta_\mu^1 \delta_\nu^0), & v > v_0, \\ \left( \frac{(D-2)(D-3)}{2} \right)^{1/2} \frac{\delta v^{D-3}}{r} (\delta_\mu^0 \delta_\nu^1 - \delta_\mu^1 \delta_\nu^0), & 0 \leq v \leq v_0, \\ 0, & v < 0, \end{cases} \\ \mu &= \begin{cases} \frac{(D-2)(D-3)\delta^2 y^{D-4}}{8\pi G_D r^2} (y_c^{D-3} - y^{D-3}), & 0 \leq v \leq v_0, \\ 0, & \text{otherwise,} \end{cases} \end{aligned} \quad (6.3)$$

where

$$y \equiv \frac{v}{r}, \quad y_c \equiv \left( \frac{\lambda}{\delta^2} \right)^{1/(D-3)}. \quad (6.4)$$

From Eqs.(5.4)-(5.7) we can see that the Ricci tensor contains only the first order derivatives of  $f$  with respect to  $v$ . Thus, there would be no matter shell to appear on a hypersurface  $v = Const.$ , as long as  $f(v, r)$  is continuous across this surface. Clearly, this is the case for the choice of Eq.(6.2) crossing the hypersurfaces  $v = 0$  and  $v = v_0$ .

When  $k = 1$ ,  $\Lambda = 0 = \delta$ , and  $X^{D-2} = S^{D-2}$ , the corresponding solution is the Vaidya solution in  $D$ -dimensional spherically symmetric spacetime [22], and was studied independently in [23,24]. In particular, da Rocha showed that when  $\lambda > \lambda_c$  the collapse always forms black holes, and when  $\lambda < \lambda_c$  the collapse always forms naked singularities, where

$$\lambda_c \equiv \frac{(D-3)^{D-3}}{[2(D-2)]^{D-2}}. \quad (6.5)$$

This result can be easily generalized to the case where  $\Lambda \neq 0$ ,  $\delta = 0$  and  $X^{D-2}$  has a topology rather than  $S^{D-2}$ . As a matter of fact, the case with  $k = 1$ ,  $\Lambda > 0$ ,  $\delta = 0$  and  $X^{D-2} = S^{D-2}$  was already studied in [25], from which we can see that Eq.(6.4) is also valid for any  $\Lambda$  and other topologies for  $X^{D-2}$  but still with  $k = 1$ ,  $\delta = 0$ .

When  $k = 1$ ,  $\Lambda = 0$ ,  $\delta \neq 0$  and  $D = 4$ , Lake and Zannias found that the collapse can form either black holes or naked singularities [26]. Ghosh generalized these results to the case where  $\Lambda > 0$  [27]. From the analysis given in these two articles one can see that the cosmological constant actually has no effects on the final state of the collapse. Therefore, the results obtained by Lake and Zannias are actually valid for any  $\Lambda$ . In addition, following their analysis it is not difficult to be convinced that *gravitational collapse of a charged Type II fluid in a higher dimensional de Sitter ( $\Lambda > 0$ ) or anti-de Sitter ( $\Lambda < 0$ ) spacetime with  $k = 1$  can form either black holes or naked singularities, depending on the choice of  $\lambda$  and  $\delta$ .*

Therefore, in the following we shall consider only the cases where  $k = 0, -1$ . Let us first consider the case  $\delta = 0$ , i.e., the collapse of a neutral null dust fluid. In this case from Eq.(5.19) we can see that to have  $f(v, r)$  be positive at least in some regions of the spacetime, we have to assume that  $\Lambda < 0$ . Then, Eq.(5.19) can be written as

$$f(v, r) = 2\lambda \left[ \frac{|\Lambda|}{2\lambda} (r^2 - r_0^2) - y^{D-3} \right],$$

$$r_0 \equiv \left| \frac{k}{\Lambda} \right|^{1/2}, \quad (6.6)$$

while Eq.(A.17) yields,

$$\theta_t \theta_n = \frac{2\lambda FG}{r^{D-1}} \left( v^{D-3} - \frac{|\Lambda|}{2\lambda} r^{D-3} (r^2 - r_0^2) \right)$$

$$= \begin{cases} < 0, & v < v_{AH}(r), \\ = 0, & v = v_{AH}(r), \\ > 0, & v > v_{AH}(r), \end{cases} \quad (6.7)$$

where

$$v_{AH}(r) \equiv r \left\{ \frac{|\Lambda|}{2\lambda} (r^2 - r_0^2) \right\}^{1/(D-3)}. \quad (6.8)$$

Thus, in the present case the  $(D-2)$ -surfaces of constant  $v$  and  $r$  are trapped in the region  $v > v_{AH}(r)$ . The hypersurface  $v = v_{AH}(r)$  represents an apparent horizon [cf. Fig. 12]. Since the spacetime singularity at  $r = 0$  starts to be formed only at the moment  $v = 0$ , from Fig. 12 we can see that this singularity is always covered by the apparent horizon. This can be seen further by studying “outgoing” null geodesics, which are given by

$$\frac{dv}{dy} = \frac{2}{|\Lambda|r^2 - |k| - 2\lambda y^{D-3}}. \quad (6.9)$$

At the moment  $v = 0$  if there exist out-going null geodesics from the point  $(v, r) = (0, 0)$ , we can see that the singularity formed at that moment will be at least locally naked. The existence of such null geodesics is characterized by the existence of positive roots of the equation [28],

$$2\lambda y_0^{D-2} + |k|y_0 + 2 = 0, \quad (6.10)$$

where

$$y_0 \equiv \lim_{v,r \rightarrow 0} \frac{v}{r} = \lim_{v,r \rightarrow 0} \frac{dv}{dr}. \quad (6.11)$$

Since all the coefficients of Eq.(6.10) are positive, no positive roots exist. As a result, the collapse will always form black holes with non-trivial topology. This generalizes the results obtained in four-dimensional case [10] to the one with any dimensions.

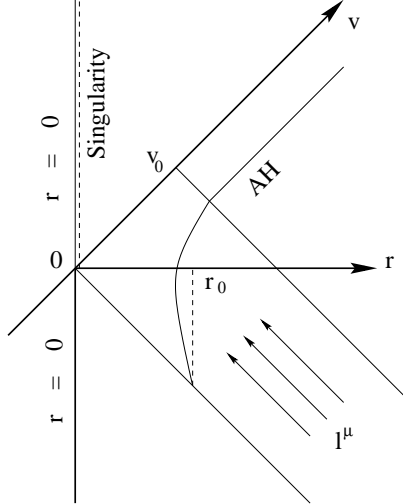


FIG. 12. Collapsing Type II fluid described by Eq.(6.2) in the text with  $k \leq 0$ ,  $\delta = 0$ , and  $\Lambda < 0$ . The curved line AH represent an apparent horizon, and the collapse always forms black holes.

When  $\delta \neq 0$ , Eq.(6.10) should be replaced by

$$\delta^2 y_0^{2D-5} - 2\lambda y_0^{D-2} - |k|y_0 - 2 = 0. \quad (6.12)$$

It is important to note that in the present case the charged fluid satisfies the weak energy condition only in the region  $y \leq y_c$ , as we can see from Eq.(6.3). On the hypersurface  $y = y_c$  the energy density becomes zero. Afterwards, the Lorentz force will push the fluid particles to move outwards [29]. As a result, the particles actually cannot enter into the region  $y > y_c$  [cf. Fig. 13]. Now to see if the spacetime singularity formed at  $(v, r) = (0, 0)$  is naked or not, one needs not only to show that a positive root of Eq.(6.12) exists, but also to show that the outgoing null geodesics fall inside the region  $y \leq y_c$ , where the solution is actually valid.

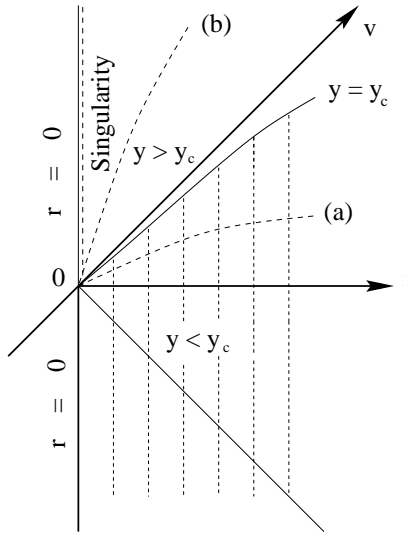


FIG. 13. Null geodesics for collapsing Type II fluid described by Eq.(6.2) with  $\delta \neq 0$ . The dashed line (a) represents an outgoing null geodesic with  $y_0^s < y_c$ , while the one (b) an outgoing null geodesic with  $y_0^s > y_c$ , where  $y_0^s$  denotes the positive root of Eq.(6.12) and  $y_c$  is defined by Eq.(6.4).

From Fig. 13 we can see that if an outgoing null geodesic falls into the region  $y < y_c$  we must have  $y_0^s < y_c$ , and if an outgoing null geodesic falls into the region  $y > y_c$ , we must have  $y_0^s > y_c$ , where  $y_0^s$  is the smallest positive root of Eq.(6.12). Since in the region  $y > y_c$  we have  $\mu < 0$  and in a realistic model this region should be replaced by an out-going charged dust fluid. Thus, in the latter case the singularity at  $(v, r) = (0, 0)$  should not be considered as naked, but in the former case it is. Therefore, to see if the singularity is naked or not now reduces to find out if  $y_0^s < y_c$  or  $y_0^s > y_c$ . To this end, let us first consider the case  $k = 0$ , and define the function  $G(y_0)$  by

$$G(y_0) \equiv \delta^2 y_0^{2D-5} - 2\lambda y_0^{D-2} - 2, \quad (k = 0). \quad (6.13)$$

From this expression we can see that  $G'(y_0) = 0$  has two roots,  $y_0^\pm$ , given by

$$y_0^- = 0, \quad y_0^+ = \left( \frac{2\lambda(D-2)}{\delta^2(2D-5)} \right)^{1/(D-3)}, \quad (6.14)$$

and

$$\begin{aligned} G(y_0^-) &= -2, \\ G(y_0^+) &= -\frac{4\lambda^2(D-2)(D-3)}{\delta^2(2D-5)^2} y_0^{+1/(D-3)} - 2 < -2, \\ G(y_c) &= -\frac{\lambda^2}{\delta^2} \left( \frac{\lambda}{\delta^2} \right)^{1/(D-3)} - 2 < -2. \end{aligned} \quad (6.15)$$

Then, the curve of  $G(y_0)$  vs  $y_0$  must be that given by the line (a) in Fig. 14, from which we can see that

$$y_0^s > y_c. \quad (6.16)$$

That is, in the present case there does not exist outgoing null geodesics in the region  $y \leq y_c$ . So, the singularity formed at the point  $(v, r) = (0, 0)$  is not naked.

When  $k = -1$ , setting

$$F(y_0) \equiv \delta^2 y_0^{2D-5} - 2\lambda y_0^{D-2} - y_0 - 2, \quad (k = -1), \quad (6.17)$$

we find that

$$G(y_0) - F(y_0) = y_0, \quad (6.18)$$

and the curve of  $F(y_0)$  vs  $y_0$  must be given by the dashed line (b) in Fig. 14. From there we can see clearly that Eq.(6.16) also holds for  $k = -1$ .

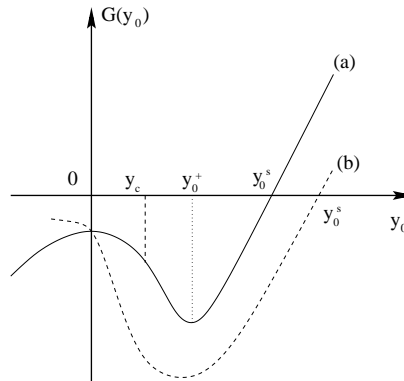


FIG. 14. (a) The function of  $G(y_0)$  defined by Eq.(6.13) for  $k = 0$ . (b) The function of  $F(y_0)$  defined by Eq.(6.17) for  $k = -1$ .

Therefore it is concluded that the *gravitational collapse of a charged null dust fluid given by Eqs.(5.19), (6.1) and (6.2) with  $k = 0$  or  $k = -1$  always forms black holes*. This is in contrast to the results obtained in [27]. The reason is that in [27] the author didn't consider the energy condition of the charged null dust fluid.

## VII. CONCLUSIONS

In this paper, we have studied topological black holes and their formation from gravitational collapse of a Type II fluid in  $D$ -dimensional spacetimes described by the metric Eq.(2.1). After presenting a general  $R^2 \times X^{D-2}$  decomposition in Sec. II, we have re-derived the charged solutions coupled with a cosmological constant, given by Eq.(3.21), in Sec. III. From their derivations we can see that these solutions are the most general ones for the spacetimes described by Eq.(2.1).

In Sec. IV, we have systematically studied the global structure of the spacetime for  $k_D = 0$  and  $D = 4$ , that is, four-dimensional spacetimes with flat topology of the  $X^2$  sector, which can be a two-dimensional plane, cylinder, Möbius band, torus, or Klein bottle, depending on how to identify the two coordinates in  $X^2$  [13]. All the corresponding Penrose diagrams have been given. In particular, it has been found that the solution with  $\Lambda < 0$  and  $q = 0$  has a black hole structure quite similar to the Schwarzschild black hole [cf. Fig. 9]. In the case where  $\Lambda < 0$ ,  $bq \neq 0$ , the global structure of the corresponding spacetime is quite similar to the Reissner-Nordström solution, including the extreme case [cf. Figs. 10 and 11].

In Sec. V, all the solutions of a Type II fluid have been found, while in Sec. VI the gravitational collapse of such a fluid has been studied. When  $k = 1$  the collapse in a de Sitter or anti-de Sitter background can form either black holes or naked singularities, but when  $k = 0$  or  $k = -1$  it always form black holes. Therefore, all the black hole solutions with different topologies found in Sec. IV can be realized from the gravitational collapse of a type II fluid in  $D$ -dimensional spacetimes.

## ACKNOWLEDGMENTS

One of the authors (AW) would like to thank Nigel Goldenfeld for his valuable discussions on gravitational collapse. He would also like to express his gratitude to the Department of Physics, UIUC, for hospitality. The financial assistance from CAPES (AW), CNPq (NOS) and FAPERJ (MFAdaS) is gratefully acknowledged.

## APPENDIX: TRAPPED SURFACES AND APPARENT HORIZONS

The concept of *trapped surface* was originally from Penrose [30], who defined it as a compact spatial two-surface  $S$  in a four-dimensional spacetime, on which  $\theta_+ \theta_-|_S > 0$ , where  $\theta_{\pm}$  denote the expansions in the future-pointing null directions orthogonal to  $S$ , and the spacetime is assumed to be time-orientable, so that “future” and “past” can be assigned consistently. One may then define a past trapped surface by  $\theta_{\pm}|_S > 0$ , and a future trapped surface by  $\theta_{\pm}|_S < 0$ .

Recently, Hayward [31] generalized the above definition to the four-dimensional cylindrical spacetimes where the two-surface  $S$  is not compact but an infinitely long cylinder, and call it trapped, marginal or untrapped, according to where  $\alpha_{,\mu}$  is timelike, null or spacelike, where  $\alpha$  is defined by

$$\alpha \equiv (|\partial_z \cdot \partial_z| \cdot |\partial_\varphi \cdot \partial_\varphi|)^{1/2}, \quad (\text{A.1})$$

with  $\xi_{(z)} = \partial_z$  and  $\xi_{(\varphi)} = \partial_\varphi$  being the two killing vector in the cylindrical spacetimes. Lately, one of the present authors showed that Hayward's definition is consistent with the one defined by the expansions of the two null directions orthogonal to the two-cylinder [32].

In this Appendix, we shall generalize the above definition to the  $D$ -dimensional case described by the metric (5.2). Now let us consider the  $(D-2)$ -surface,  $S$ , of constant  $v$  and  $r$ . When  $k = 1$  it could be a  $(D-2)$ -sphere, although other topologies can also exist. When  $k \neq 1$  it can be compact or non-compact, depending on how to identify the coordinates in  $S$ . For more details, we refer readers to [13,33] and references therein.

To calculate the expansions of the two null directions orthogonal to the  $(D-2)$ -surface  $S$  of constant  $x^a$  in the metric (5.2), it is found convenient to introduce two null coordinates  $\bar{v}$  and  $\bar{u}$  via the relations

$$\begin{aligned} d\bar{u} &= G(v, r) (fe^\psi dv + 2\epsilon dr), \\ d\bar{v} &= F(v)dv, \end{aligned} \quad (\text{A.2})$$

or inversely

$$\begin{aligned} dr &= \frac{\epsilon}{2} \left( \frac{1}{G} d\bar{u} - \frac{1}{F} f e^\psi d\bar{v} \right), \\ dv &= \frac{1}{F} d\bar{v}, \end{aligned} \quad (\text{A.3})$$

where  $G(v, r)$  is determined by the integrability condition  $\bar{u}_{,vr} = \bar{u}_{,rv}$ , and  $F(v)$  is an arbitrary function of  $v$  only. Without loss of generality we shall assume that they are all strictly positive,

$$F(v) > 0, \quad G(v, r) > 0. \quad (\text{A.4})$$

Then, in terms of  $\bar{u}$  and  $\bar{v}$  the metric (5.2) takes the form

$$ds^2 = -2e^{2\sigma} d\bar{u}d\bar{u} + r^2 h_{AB} (x^C) dx^A dx^B, \quad (\text{A.5})$$

where  $\sigma$  and  $r$  are now the functions of  $\bar{u}$  and  $\bar{v}$  via Eq.(A.2) and

$$\sigma \equiv \frac{1}{2} [\psi - \ln(2FG)]. \quad (\text{A.6})$$

Clearly, the metric (A.5) is invariant under the coordinate transformations

$$\bar{u} = \bar{u}(\tilde{u}), \quad \bar{v} = \bar{v}(\tilde{v}). \quad (\text{A.7})$$

Using this gauge freedom, we shall assume that metric (A.5) is free of coordinate singularities. Then, it can be shown that

$$\begin{aligned} {}^{(2)}R_{ab} &= -2\sigma_{,\bar{u}\bar{v}} (\delta_a^0 \delta_b^1 + \delta_a^1 \delta_b^0), \\ \nabla_a \nabla_b r &= r_{,ab} - 2 (\sigma_{,\bar{u}r, \bar{u}} \delta_a^0 \delta_b^0 + \sigma_{,\bar{v}r, \bar{v}} \delta_a^1 \delta_b^1). \end{aligned} \quad (\text{A.8})$$

Substituting Eq.(A.8) into Eq.(2.7) we find that

$$\begin{aligned} {}^{(D)}R_{\bar{u}\bar{u}} &= -\frac{D-2}{r} (r_{,\bar{u}\bar{u}} - 2\sigma_{,\bar{u}} r_{,\bar{u}}), \\ {}^{(D)}R_{\bar{u}\bar{v}} &= -2\sigma_{,\bar{u}\bar{v}} - \frac{D-2}{r} r_{,\bar{u}\bar{v}}, \\ {}^{(D)}R_{\bar{v}\bar{v}} &= -\frac{D-2}{r} (r_{,\bar{v}\bar{v}} - 2\sigma_{,\bar{v}} r_{,\bar{v}}), \\ {}^{(D)}R_{AB} &= \{k_D + 2e^{-2\sigma} [rr_{,\bar{u}\bar{v}} + (D-3)r_{,\bar{u}}r_{,\bar{v}}]\} h_{AB}. \end{aligned} \quad (\text{A.9})$$

On the other hand, introducing two null vectors  $l_\mu$  and  $n_\mu$  by

$$l_\lambda \equiv \frac{\partial \bar{u}}{\partial x^\lambda} = \delta_{\bar{u}}^\lambda, \quad n_\lambda \equiv \frac{\partial \bar{v}}{\partial x^\lambda} = \delta_{\bar{v}}^\lambda, \quad (\text{A.10})$$

one can see that the two null vectors are future directed, and orthogonal to the  $(D-2)$ -surface,  $S$ , of constant  $\bar{u}$  and  $\bar{v}$  (or constant of  $v$  and  $r$ ). In addition, each of them defines an affinely parametrized null geodesic congruence, since now the following holds

$$\begin{aligned} \frac{D}{D\lambda} l^\mu &= l^\mu{}_{;\nu} l^\nu = 0, \\ \frac{D}{D\delta} n^\mu &= n^\mu{}_{;\nu} n^\nu = 0, \end{aligned} \quad (\text{A.11})$$

where a semicolon “;” denotes the covariant derivative with respect to  $g_{\mu\nu}$ , and  $\lambda$  and  $\delta$  the affine parameters along the null rays defined, respectively, by  $l^\mu$  and  $n^\mu$  (It should be noted that the symbol  $\delta$  used here should not be confused with the one used in Eq.(6.2) for the charge density.). In particular,  $l^\mu$  defines the one moving along the null hypersurfaces  $\bar{u} = \text{Const.}$ , while  $n^\mu$  defines the one moving along the null hypersurfaces  $\bar{v} = \text{Const.}$  Then, the expansions of these null geodesics are defined by [18],



$$\begin{aligned}\theta_l &\equiv -\frac{1}{D}g^{\alpha\beta}l_{\alpha;\beta} = e^{-2\sigma}\frac{r_{,\bar{v}}}{r}, \\ \theta_n &\equiv -\frac{1}{D}g^{\alpha\beta}n_{\alpha;\beta} = e^{-2\sigma}\frac{r_{,\bar{u}}}{r}.\end{aligned}\tag{A.12}$$

Thus, we have

$$\theta_l\theta_n = e^{-4\sigma}\frac{r_{,\bar{v}}r_{,\bar{u}}}{r^2} = -\frac{1}{2r^2}e^{-2\sigma}r_{,\alpha}r^{,\alpha}.\tag{A.13}$$

It should be noted that the affine parameter  $\lambda$  (or  $\delta$ ) is unique only up to a function  $f^{-1}(\bar{u})$  (or  $g^{-1}(\bar{v})$ ), which is a constant along each curve  $\bar{u} = \text{Const.}$  (or  $\bar{v} = \text{Const.}$ ) [18]. In fact,  $\bar{\lambda} = \lambda/f(\bar{u})$  ( $\bar{\delta} = \delta/g(\bar{v})$ ) is another affine parameter and the corresponding tangent vectors are

$$\bar{l}_\mu = f(\bar{u})\delta_\mu^{\bar{u}}, \quad \bar{n}_\mu = g(\bar{v})\delta_\mu^{\bar{v}},\tag{A.14}$$

and the corresponding expansions are given by

$$\bar{\theta}_{\bar{l}} = f(\bar{u})\theta_l, \quad \bar{\theta}_{\bar{n}} = g(\bar{v})\theta_n.\tag{A.15}$$

However, since along each curve  $\bar{u} = \text{Const.}$  (or  $\bar{v} = \text{Const.}$ ) the function  $f(\bar{u})$  (or  $g(\bar{v})$ ) is constant, this does not affect our definition of trapped surfaces in terms of the expansions. Thus, without loss of generality, in the following we consider only the expressions given by Eq.(A.12).

Once we have the expansions, following Penrose we can define that a  $(D-2)$ -surface,  $S$ , of constant  $\bar{u}$  and  $\bar{v}$  is trapped, marginally trapped, or untrapped, according to whether  $\theta_l\theta_n > 0$ ,  $\theta_l\theta_n = 0$ , or  $\theta_l\theta_n < 0$ . An apparent horizon, or trapping horizon in Hayward's terminology [31], is defined as a hypersurface foliated by marginally trapped surfaces.

Since  $e^{-2\sigma}$  is regular, except at some points or surfaces on which the spacetime is singular, from Eq.(A.13) we can see that trapped, marginally trapped, or untrapped surfaces can be also defined according to whether  $r_{,\alpha}$  is timelike, null, or spacelike.

On the other hand, from Eq.(A.3) we find that

$$\frac{\partial r}{\partial \bar{u}} = \frac{\epsilon}{2G}, \quad \frac{\partial r}{\partial \bar{v}} = -\frac{\epsilon f}{2F}e^\psi.\tag{A.16}$$

Inserting the above expressions into Eq.(A.12) we obtain

$$\begin{aligned}\theta_l &\equiv -\frac{1}{D}g^{\alpha\beta}l_{\alpha;\beta} = e^{-2\sigma}\frac{r_{,\bar{v}}}{r}, \\ &= -\frac{\epsilon f}{2rF}e^{\psi-2\sigma}, \\ \theta_n &\equiv -\frac{1}{D}g^{\alpha\beta}n_{\alpha;\beta} = e^{-2\sigma}\frac{r_{,\bar{u}}}{r} \\ &= \frac{\epsilon}{2rG}e^{-2\sigma}, \\ \theta_l\theta_n &= -\frac{FG}{r^2}fe^{-\psi}.\end{aligned}\tag{A.17}$$

- [1] J. Maldacena, Adv. Theor. Math. Phys. **2**, 231 (1998); E. Witten, *ibid.*, **2**, 253 (1998); O. Aharony, S.S. Gubser, J. Maldacena, H. Ooguri, and Y. Oz, Phys. Rep. **323**, 183 (2000).
- [2] S. Dimopoulos and G. Landsberg, Phys. Rev. Lett. **87**, 161602 (2001); S.B. Giddings and S. Thomas, Phys. Rev. **D65**, 056010 (2002).
- [3] S.W. Hawking, Commun. Math. Phys. **25**, 152 (1972).
- [4] J. L. Friedman, K. Schleich, and D. M. Witt, Phys. Rev. Lett. **71**, 1486 (1993); *ibid.*, **75**, 1872(E) (1993); G. Galloway, K. Schleich, D. Witt, and E. Woolgar, Phys. Rev. **D60**, 104039 (1999); M. Cai, and G.J. Galloway, Class. Quantum Grav. **18**, 2707 (2001), and references therein.

- [5] C. Huang and C. Liang, Phys. Lett. **A201** 27, (1995); J. Lemos, Phys. Lett. **B353**, 46 (1995); R. Cai and Y. Zhang, Phys. Rev. **D54**, 4891 (1996); R.B. Mann, Class. Quantum Grav. **14**, L109 (1997); D. R. Brill, J. Louko, and P. Peldan, Phys. Rev. **D56**, 3600 (1997); L. Vanzo, *ibid.*, **D56**, 6475 (1997); R.G. Cai, J. Ji and K. Soh, *ibid.*, **D57**, 6547 (1998); D. Klemm, Class. Quant. Grav. **15**, 3195 (1998); D. Klemm, V. Moretti and L. Vanzo, Phys. Rev. **D57**, 6127 (1998).
- [6] R.C. Myers and M.J. Perry, Ann. Phys. (N.Y.) **172**, 304 (1986).
- [7] R. Emparan and H.S. Reall, Phys. Rev. Lett. **88**, 101101 (2002).
- [8] G.W. Gibbons, D. Ida, and T. Shiromizu, Phys. Rev. Lett. **89**, 041101 (2002); Prog. Theor. Phys. Suppl. **148**, 284 (2003).
- [9] S. Aminneborg, I. Bengtsson, S. Holst, and P. Peldan, Class. Quant. Grav. **13**, 2707 (1996); M. Banados, A. Gomberoff and C. Martinez, *ibid.*, **15**, 3575 (1998); M. Banados, Phys. Rev. **D57**, 1068 (1998); D. Birmingham, Class. Quant. Grav. **16**, 1197 (1999); R.G. Cai and K.S. Soh, Phys. Rev. **D59**, 044013 (1999).
- [10] W.L. Smith and R.B. Mann, Phys. Rev. **D56**, 4942 (1997); R.G. Cai, L.Z. Qiao, and Y.Z. Zhang, Mod. Phys. Lett. **A12**, 155 (1997); J. Lemos, Phys. Rev. **D57**, 4600 (1998).
- [11] A. Banerjee, A. Sil, and S. Chatterjee, Astrophys. J. **422**, 681 (1994); J.F.V. da Rocha and A.Z. Wang, “*Gravitational Collapse of Perfect Fluid in N-dimensional Spherically Symmetric Spacetimes*,” gr-qc/9910109 (1999); Class. Quantum Grav. **17**, 2589 (2000); S.G. Ghosh and A. Beesham, Phys. Rev. **D64**, 124005 (2001); A. Banerjee, U. Debnath, and S. Chakraborty, “*Naked Singularities in Higher Dimensional Gravitational Collapse*,” gr-qc/0211099 (2002); U. Debnath and S. Chakraborty, “*Gravitational Collapse in Higher Dimension*,” gr-qc/0211102 (2002); R. Goswami and P.S. Joshi, “*Is Cosmic Censorship Valid in Higher Dimensions*,” gr-qc/0212097 (2002); S.G. Ghosh and D.W. Deshkar, “*Gravitational Collapse of Perfect Fluid in Self-Similar Higher Dimensional Spacetimes*,” gr-qc/0304075, to appear in Int. J. Mod. Phys. (2003), and references therein.
- [12] R.-G. Cai and K.-S. Soh, Phys. Rev. **D59**, 044013 (1999).
- [13] J.A. Wolf, *Spaces of Constant Curvature* (McGraw-Hill, New York, 1967).
- [14] I.D. Novikov and V.P. Frolov, *Physics of Black Holes* (Kluwer Academic Publishers, London, 1989), pp.256-265.
- [15] M. Cvetič, S. Griffies, and H.H. Soleng, Phys. Rev. **D48**, 2613 (1993).
- [16] M. Walker, J. Math. Phys. **11**, 2280 (1970).
- [17] A.H. Taub, Ann. Math. **53**, 472 (1951).
- [18] S.W. Hawking and G.F.R. Ellis, *The Large Scale Structure of Space-Time* ( Cambridge University Press, Cambridge, England, 1973).
- [19] B. Carter, Phys. Lett. **21**, 423 (1966).
- [20] V. Husian, Phys. Rev. **D53**, R1759 (1996).
- [21] A.Z. Wang and Y. Wu, Gen. Relativ. Grav. **31**, 107 (1999).
- [22] L.K. Patel and N. Dadhich, “*Exact solutions for null fluid collapse in high dimensions*,” gr-qc/9909068, unpublished (1999).
- [23] S.G. Ghosh and N. Dadhich, Phys. Rev. **D64**, 047501 (2001).
- [24] J.F.V. da Rocha, In. J. Mod. Phys. **D11**, 113 (2002).
- [25] S.G. Ghosh and N. Dadhich, Phys. Rev. **D65**, 127502 (2002).
- [26] K. Lake and T. Zannias, Phys. Rev. **D43**, 1798 (1991).
- [27] S.G. Ghosh, Phys. Rev. **D62**, 127505 (2002).
- [28] P.S. Joshi, *Global Aspects in Gravitation and Cosmology* (Clarendon, Oxford, 1993).
- [29] A. Ori, Class. Quantum Grav. **8**, 1559 (1991).
- [30] R. Penrose, in *Batelle Rencontres*, edited by C.M. DeWitt and B.S. DeWitt (Gordon and Breach, New York, 1968).
- [31] S.A. Hayward, Phys. Rev. **D49**, 6467 (1994); Class. Quantum Grav. **17**, 1749 (2000).
- [32] A.Z. Wang, *Comment on “Absence of trapped surfaces and singularities in cylindrical collapse*,” to be published (2003).
- [33] G. Gibbons and S.A. Hartnoll, Phys. Rev. **D66**, 064024 (2002), and references therein.